AFAPL-TR-71-95

DEVELOPMENT AND CALIBRATION OF A MACH 1.5 SAND EROSION TEST APPARATUS

DENNIS R. PANDY, CAPT, USAF

TECHNICAL REPORT AFAPL-TR-71-95

MARCH 1972

AIR FORCE AERO PROPULSION LABORATORY
AIR FORCE SYSTEMS COMMAND
WRIGHT-PATTERSON AIR FORCE BASE, OHIO 45433

69

NOTICE

When Government drawings, specifications, or other data are used for any purpose other than in connection with a definitely related Government procurement operation, the United States Government thereby incurs no responsibility nor any obligation whatsoever; and the fact that the government may have formulated, furnished, or in any way supplied the said drawings, specifications, or other data, is not to be regarded by implication or otherwise as in any manner licensing the holder or any other person or corporation, or conveying any rights or permission to manufacture, use, or sell any patented invention that may in any way be related thereto.

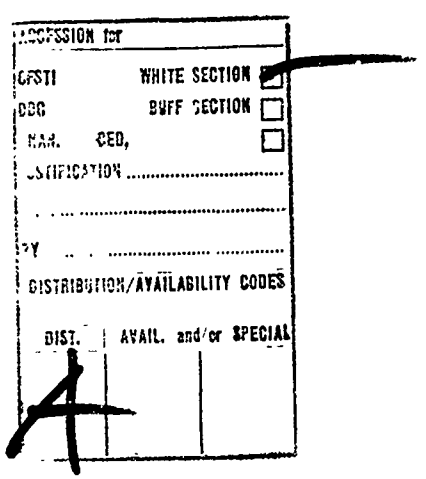

Copies of this report should not be returned unless return is required by security considerations, contractual obligations, or notice on a specific document.

AIR FORCE: 31-5-72/50

UNCLASSIFIED

Security Classification

DOCUMENT CONTROL DATA - R & D

(Security classification of title, body of abstract and indexing annotation must be entered when the overall report is classified)

1. ORIGINATING ACTIVITY (Corporate author)	2a. REPORT SECURITY CLASSIFICATION
Air Force Aero Propulsion Laboratory Wright-Patterson Air Force Base, Ohio 45433	UNCLASSIFIED
	2b. GROUP

3 REPORT TITLE

DEVELOPMENT AND CALIBRATION OF A MACH 1.5 SAND EROSION TEST APPARATUS

4. DESCRIPTIVE NOTES (Type of report and inclusive dates)

5 AUTHOR(S) (First name, middle initial, last name)

Dennis R. Pandy, Capt, USAF

6. REPORT DATE	7a. TOTAL NO OF PAGES	7b. NO OF REFS
March 1972	69	5

8a. CONTRACT OR GRANT NO.	9a. ORIGINATOR'S REPORT NUMBER(S)
b. PROJECT NO. 3066	AFAPL-TR-71-95
c. 03	9b. OTHER REPORT NO(S) (Any other numbers that may be assigned this report)
d. 043	

10 DISTRIBUTION STATEMENT

Approved for public release; distribution unlimited.

11. SUPPLEMENTARY NOTES	12. SPONSORING MILITARY ACTIVITY
	Air Force Aero Propulsion Laboratory Wright-Patterson Air Force Base Ohio 45433

13 ABSTRACT

Development of a Mach 1.5 Sand Erosion Test Apparatus is described. This rotating arm apparatus is designed to simulate the erosive environment which a turbine engine fan or compressor blade would see when operating with sand or dust ingestion. It will be used to evaluate the mechanisms of sand erosion and the relative erosion resistance of fan and compressor blade and coating materials at rotor tip speeds up to 1600 ft/sec. This report describes the design and development of the apparatus including the rotating arm, power train, test enclosure, and sand control system. Calibration and correlation experiments are also described.

DD FORM 1 NOV 68 1473

UNCLASSIFIED

Security Classification

14 KEY WORDS	LINK A		LINK B		LINK C	
	ROLE	WT	ROLE	WT	ROLE	WT
Sand Erosion Endurance Testing In-House Facility Compressor Blade Materials MIL-Spec Environment						

☆U.S.Government Printing Office: 1972 — 759-086/573

AFAPL-TR-71-95

DEVELOPMENT AND CALIBRATION OF A MACH 1.5 SAND EROSION TEST APPARATUS

DENNIS R. PANDY, CAPT, USAF

AIR FORCE AERO PROPULSION LABORATORY

FOREWORD

The work described in this report was conducted within the Propulsion Branch, Turbine Engine Division, Air Force Aero Propulsion Laboratory, Wright-Patterson Air Force Base, Ohio. The effort was accomplished under Project 3066-03-043 from September 1966 through April 1971. The author served as the Project Engineer.

The author gratefully acknowledges the assistance of Richard Warman in the design and setup of the test apparatus and the assistance of Steve Lindenbaum and Richard Hill in preparing this report.

This report was submitted by the author in September 1971.

This technical report has been reviewed and is approved.

Ernest C. Simpson

ERNEST C. SIMPSON
Director, Turbine Engine Division
Air Force Aero Propulsion Laboratory

ABSTRACT

Development of a Mach 1.5 Sand Erosion Test Apparatus is described. This rotating arm apparatus is designed to simulate the erosive environment which a turbine engine fan or compressor blade would see when operating with sand or dust ingestion. It will be used to evaluate the mechanisms of sand erosion and the relative erosion resistance of fan and compressor blade and coating materials at rotor tip speeds up to 1600 ft/sec. This report describes the design and development of the apparatus including the rotating arm, power train, test enclosure, and sand control system. Calibration and correlation experiments are also described.

TABLE OF CONTENTS

ILLUSTRATIONS

ILLUSTRATIONS (Contd)

SECTION I

INTRODUCTION

The erosion of aircraft gas turbine engine compressor blades and vanes by sand and dust ingestion has always been a problem. However, early jet-powered aircraft operated from paved runways or surfaces of low sand and dust concentrations. Consequently, the engine performance degradation was gradual and could be handled by normal time between overhaul (TBO) maintenance. Then, in the mid 1960's, the problem was brought to the foreground by extensive aircraft operations in Southeast Asia. Because of the natural environment and operational tactics, turbine engines were exposed to severe sand and dust concentrations. The resultant rapid erosion caused significant loss of engine power and compressor stall margin. Unscheduled engine removals were experienced in as little as one tenth the normal TBO, i.e. 250 hours. Such reduced engine life significantly increased the cost of operations (reportedly over one hundred million dollars per year) and limited aircraft availability. Because of the drastic increase in operational costs, immediate solutions were sought.

Three approaches were considered to solve the problem:

(1) Develop a filtration system that would remove most of the solid particles from the engine inlet air stream prior to the air entering the compression system. Filters and separators, however, have invariably decreased engine efficiency, increased engine weight, and required constant maintenance. The development of a reasonably efficient and maintenance-free filtration system would require extensive development time.

(2) Develop compressor configurations which are less susceptible to sand and dust ingestion. Unfortunately, the aerodynamic parameters that influence ingestion capabilities are also critical to efficient compressor performance. High tip speed, minimum tip clearance, and high blade loading all increase compressor erosion susceptibility, but are also important to compressor efficiency and weight. Consequently, a

compressor designed to operate in a sand and dust environment would also tend to have less than desired performance.

(3) Develop compressor blade materials that are affected minimally by sand and dust. Though this approach has not as yet effected the ultimate solution, it seems to have the greatest potential for success. Several materials with excellent erosion durability properties show great promise as erosion-resistant compressor blade coatings. These coatings have no effect on compressor weight or efficiency.

At the same time the erosion problem surfaced, composite materials were beginning to be recognized by both the Air Force and industry as having an excellent potential for turbine engine application. These materials have a high strength-to-weight ratio and elastic modulus, and therefore seem ideally suited for lightweight, high-tip-speed fan designs. However, the matrix materials commonly used, such as epoxy, polyimides, and aluminum, all have very poor erosion resistance properties. The ability of these composite materials to withstand even limited exposure to sand and dust was questioned. In order to fully identify the erosion characteristics of composites, a low cost facility was needed to test these materials in a simulated erosive environment.

To meet the needs of a composite material test facility and, simultaneously, to provide a rig to screen compressor blade materials and coatings, the Air Force Aero Propulsion Laboratory initiated the Sand Erosion Test Facility Program. The objective of this program was to develop a low cost compressor blade sand erosion test device which simulates the environment to which a turbine engine compressor blade is exposed, as outlined in military specifications MIL-E-5007C and 5009C (References 1 and 2). These specifications require an engine, for qualification purposes, to be tested for 10 hours at maximum continuous rating with a sand ingestion of 4.4×10^{-5} pounds of sand per pound of air. The size distribution of the sand particles ranges from 25 to 1000 microns, with the majority of the particles between 200 and 400 microns. The development, calibration, and checkout of the Air Force

Aero Propulsion Laboratory sand erosion test facility are discussed in the following sections of this report.

SECTION II

FACILITY DESCRIPTION

The sand erosion facility, located at Wright-Patterson AFB, Ohio, was designed to produce conditions simulating those existing where sand and dust are ingested in a turbine engine compressor. Tests are accomplished by attaching test specimens to a 15-inch arm and rotating them through a stream of sand at a representative rpm (Figure 1). The arm can be rotated at 12,000 rpm, which gives the specimens a physical tip speed velocity of 1600 ft/sec. Sand is fed into the sample's path at the desired flow rate, velocity, and impingement angle to simulate accelerated blade exposure in an operational sand and dust environment. Control of sample velocity, sand mass flow rate, sand velocity, and impingement angle allow test conditions to be reproduced with adequate precision so as to permit the mechanisms of sand and dust erosion to be thoroughly investigated.

Tests are conducted in a 4 x 8 x 8 foot chamber with oak and steel walls which can contain the test samples and rotating arm should they fail and fly free of the drive shaft. For further protection, the entire test chamber and drive train are enclosed in a heavily insulated test cell, as shown in Figure 2, to reduce the operating noise level around the facility. Maximum noise level readings in the control room adjacent to the test cell were between 85 and 88 PNdb when operating at 12,000 rpm.

From the control room, shown in Figure 3, the material specimens can be observed during test runs by closed-circuit television. The television camera is focused onto the specimens through a plexiglass window in the test chamber, as shown in Figure 4. The specimens are illuminated by a strobe light triggered by a magnetic pickup, which, in turn, reads off a 60-tooth gear on the output shaft, shown in Figure 5. Shaft rpm is also obtained from this pickup. A video tape recorder and television monitor in the control room are used as test monitors. Additional equipment in the control room permits real-time readout of

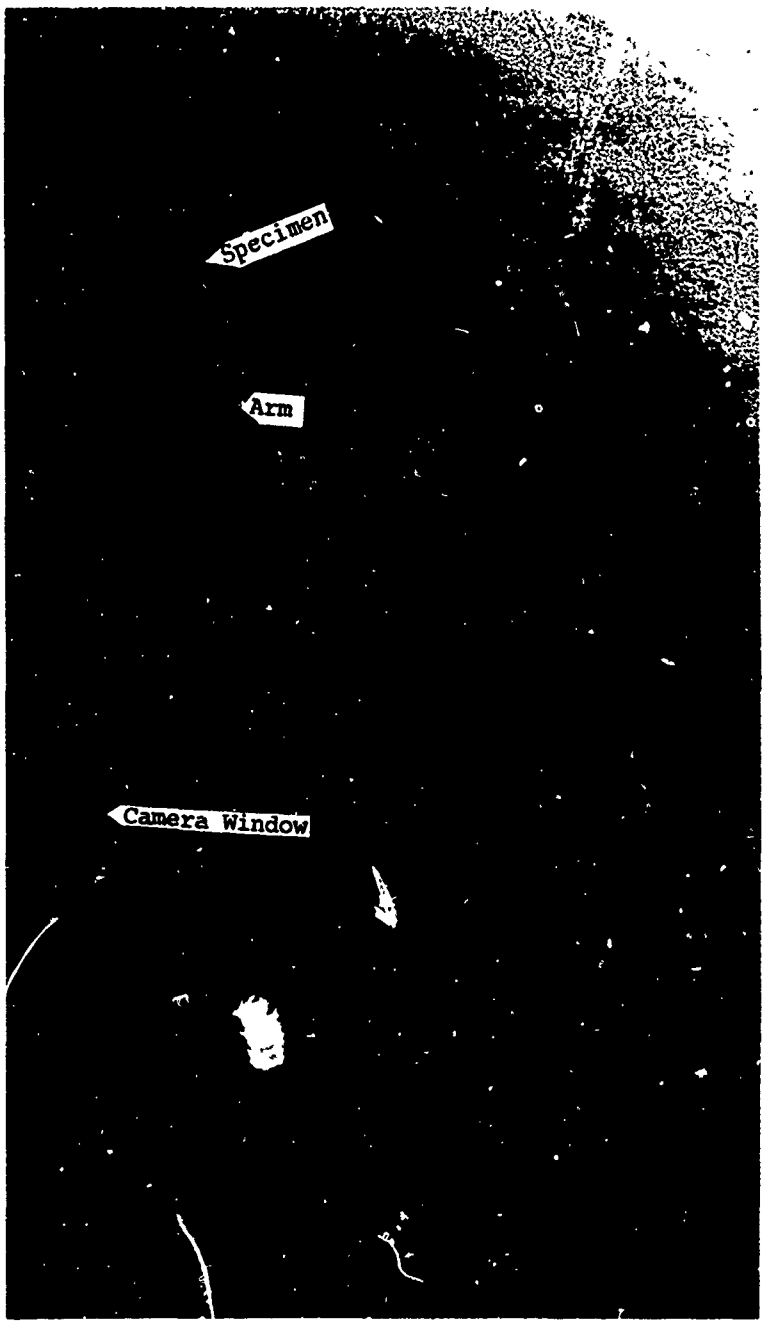

Figure 1. Rotating Arm With Specimens

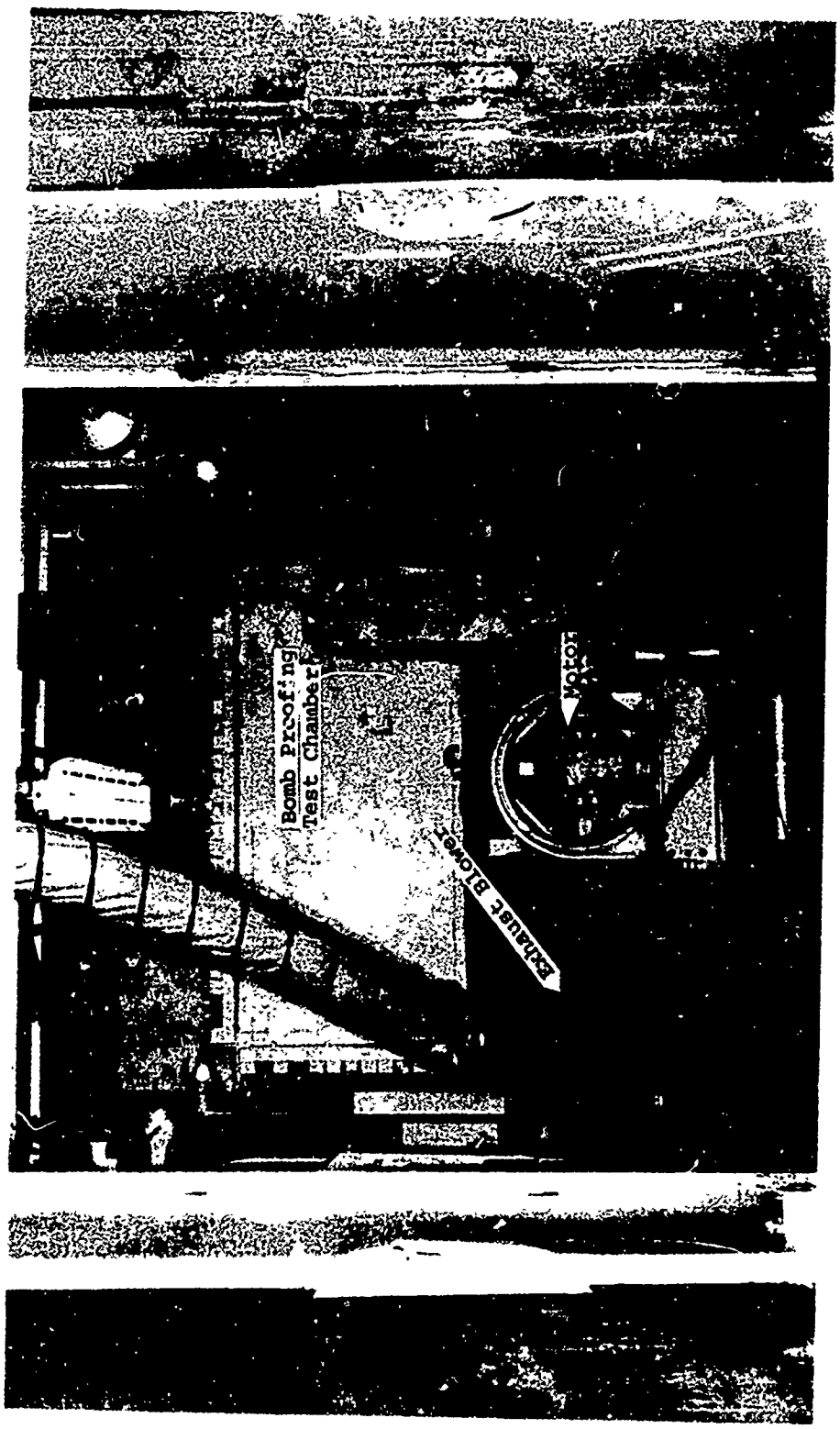

Figure 2. Entrance View of Test Cell

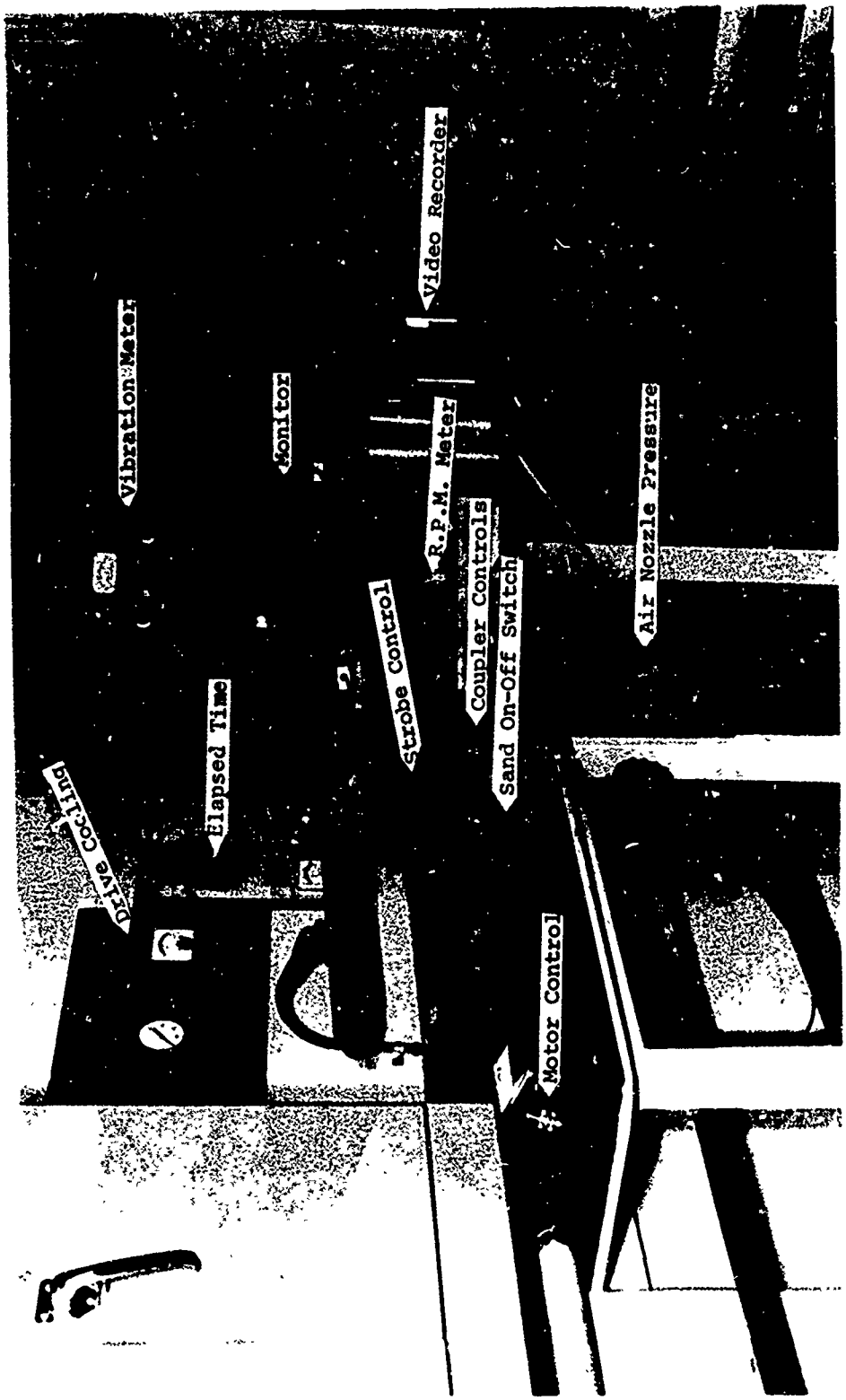

Figure 3. Control Room

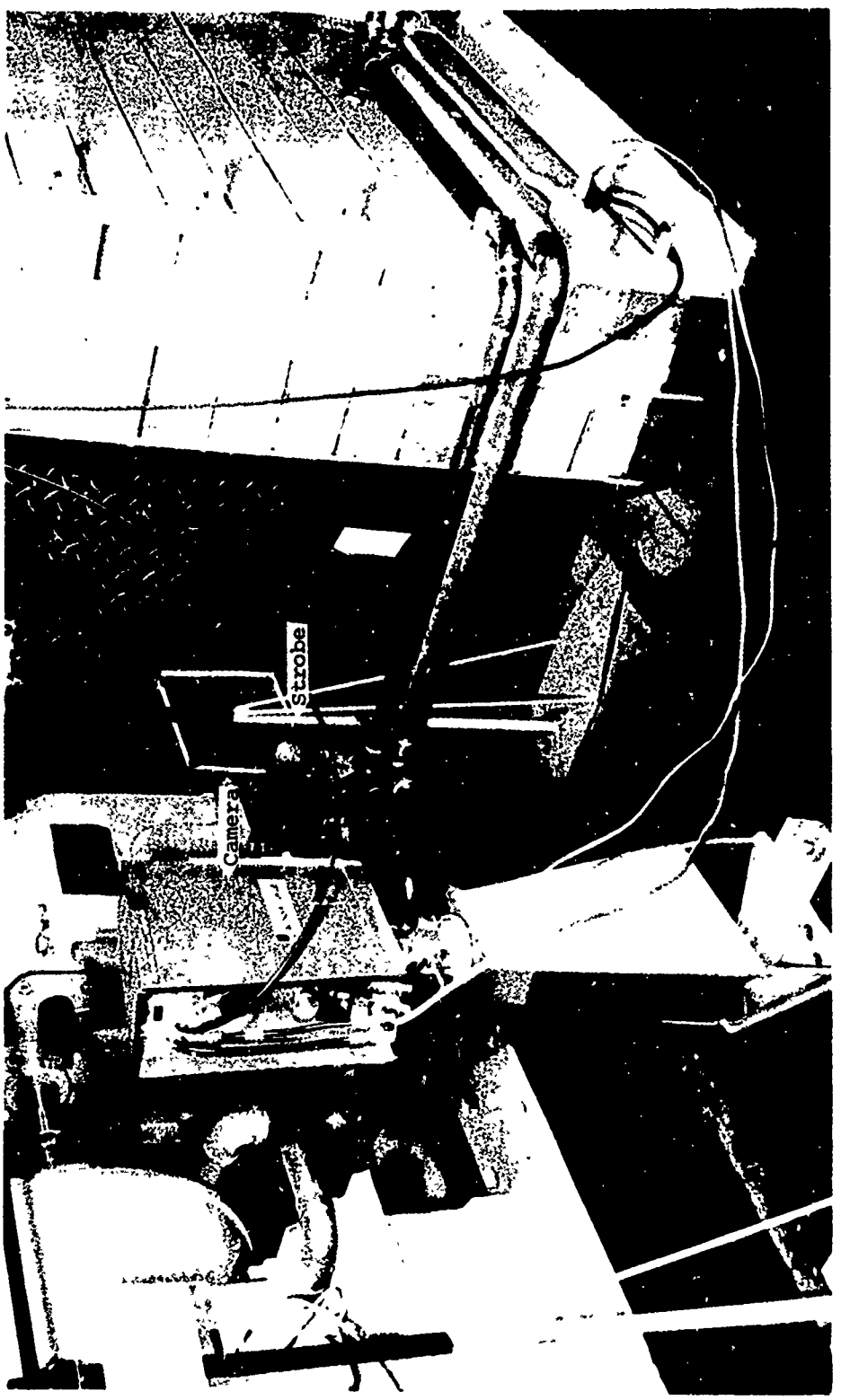

Figure 4. Television Camera Installation

Figure 5. Strobe and RPM Meter Pickup

test chamber temperature, rotating arm speed, motor loading, vertical and horizontal gearbox vibrations, gearbox oil temperature and pressure, air pressure to the sand feed mechanism, and elapsed time for sand flow.

Sand particles are blown onto the test specimens through a nozzle 1/2 inch in diameter by 7 feet long, as shown in Figure 6. The nozzle is pressurized by regulated 90 psi shop air and has been calibrated for air flows between 100 and 900 ft/sec. Sand flows into the nozzle from a pressurized hopper, which has a calibrated orifice to regulate the flow. The hopper is heated by a heat lamp to ensure that the sand is kept moisture-free prior to each test run. The sand flow is started and stopped by pinching the flexible hose connecting the hopper to the nozzle; this is done remotely from the control room with a motor-servo mechanism, shown in Figure 7.

Once sand has passed through the specimen's path, it is drawn out of the test chamber and through a filter system to prevent secondary impacts. The device for accomplishing this, shown in Figure 8, consists of a simple duct leading from the test chamber followed in series by a labyrinth separator, several dry filters, a wet filter, and an exhaust fan. The interior walls of the test chamber are smooth for easy cleaning of stray sand particles.

A second and larger exhaust fan is used to circulate cool air through the test chamber to prevent excessive heat build up. The fan, shown in Figure 9, has a 450 cfm capacity and can maintain the temperature of the test chamber below 200°F during continuous high-speed operation.

The drive train for the arm consists of a 100 HP counterwound induction motor operated at constant speed, an adjustable-speed eddy current power coupling, and a 3.483:1 speed increasing gearbox. Speed control for the output shaft is maintained with the adjustable speed coupling. This unit gives precise control of the output shaft speed between 1000 and 12,000 rpm and provides the additional safety features of power uncoupling and output shaft braking for emergency stop conditions.

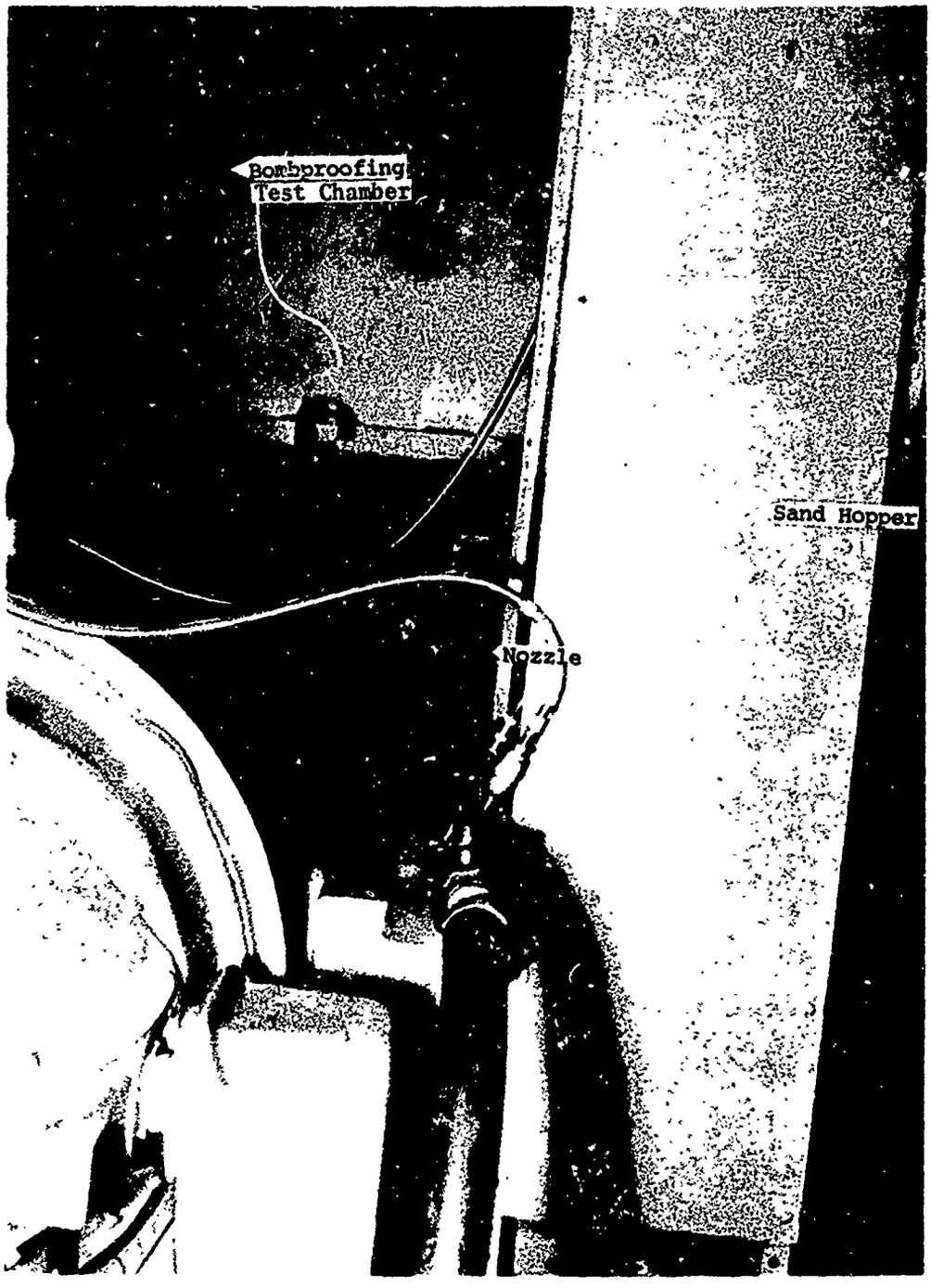

Figure 6. Looking Down Sand Nozzle

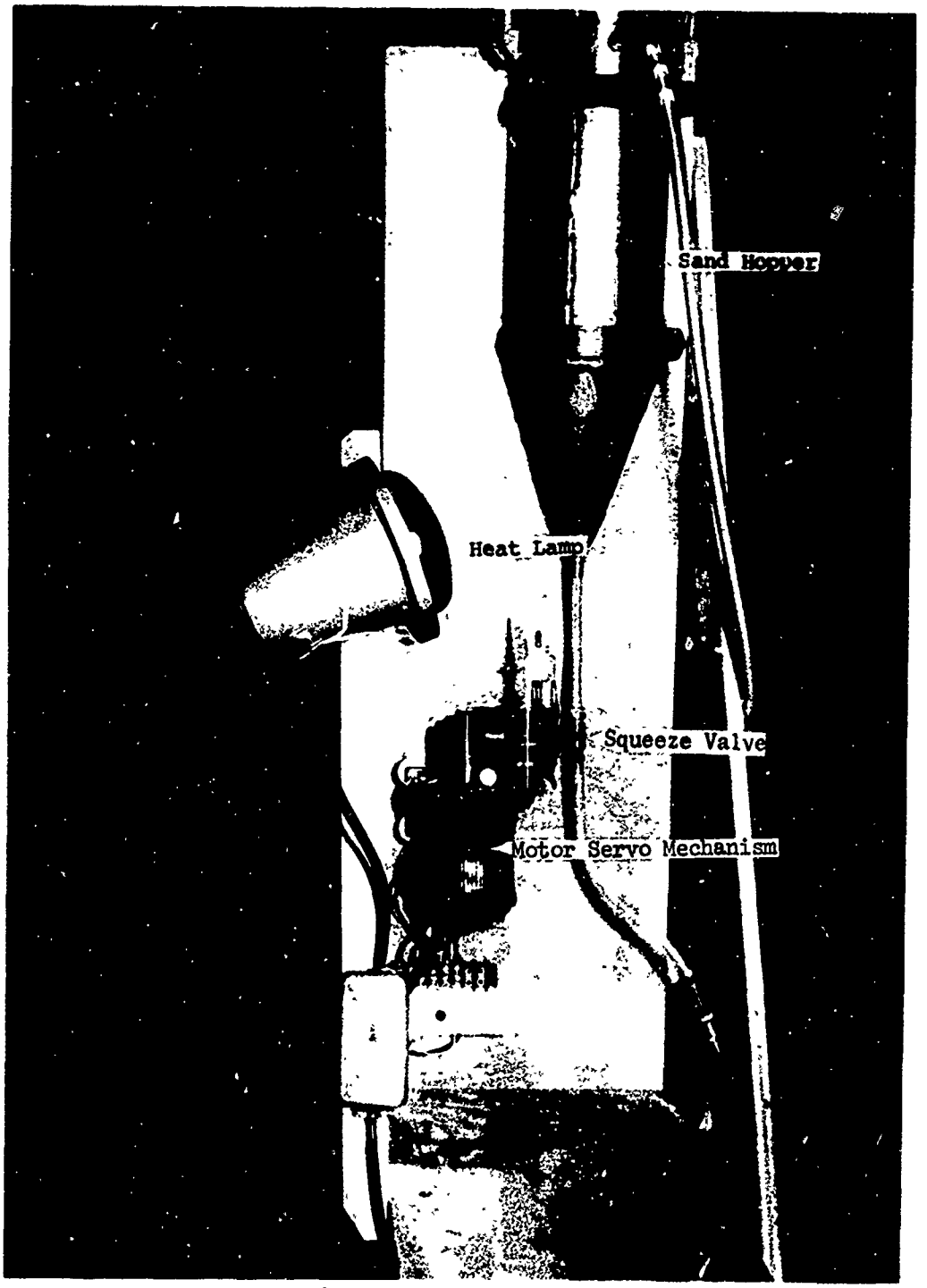

Figure 7. Sand Feed Mechanism

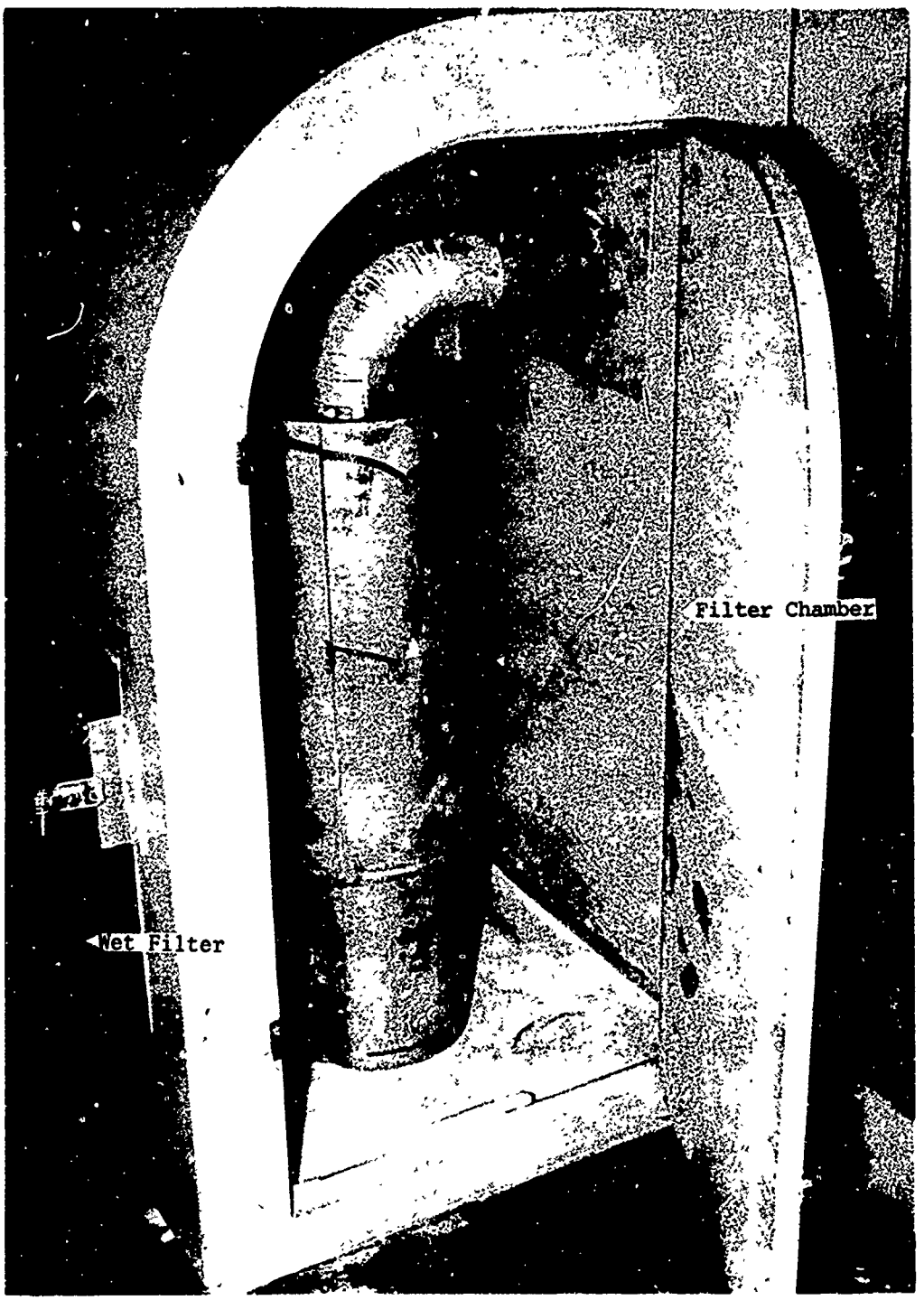

Figure 8. Sand Exhaust Filter System

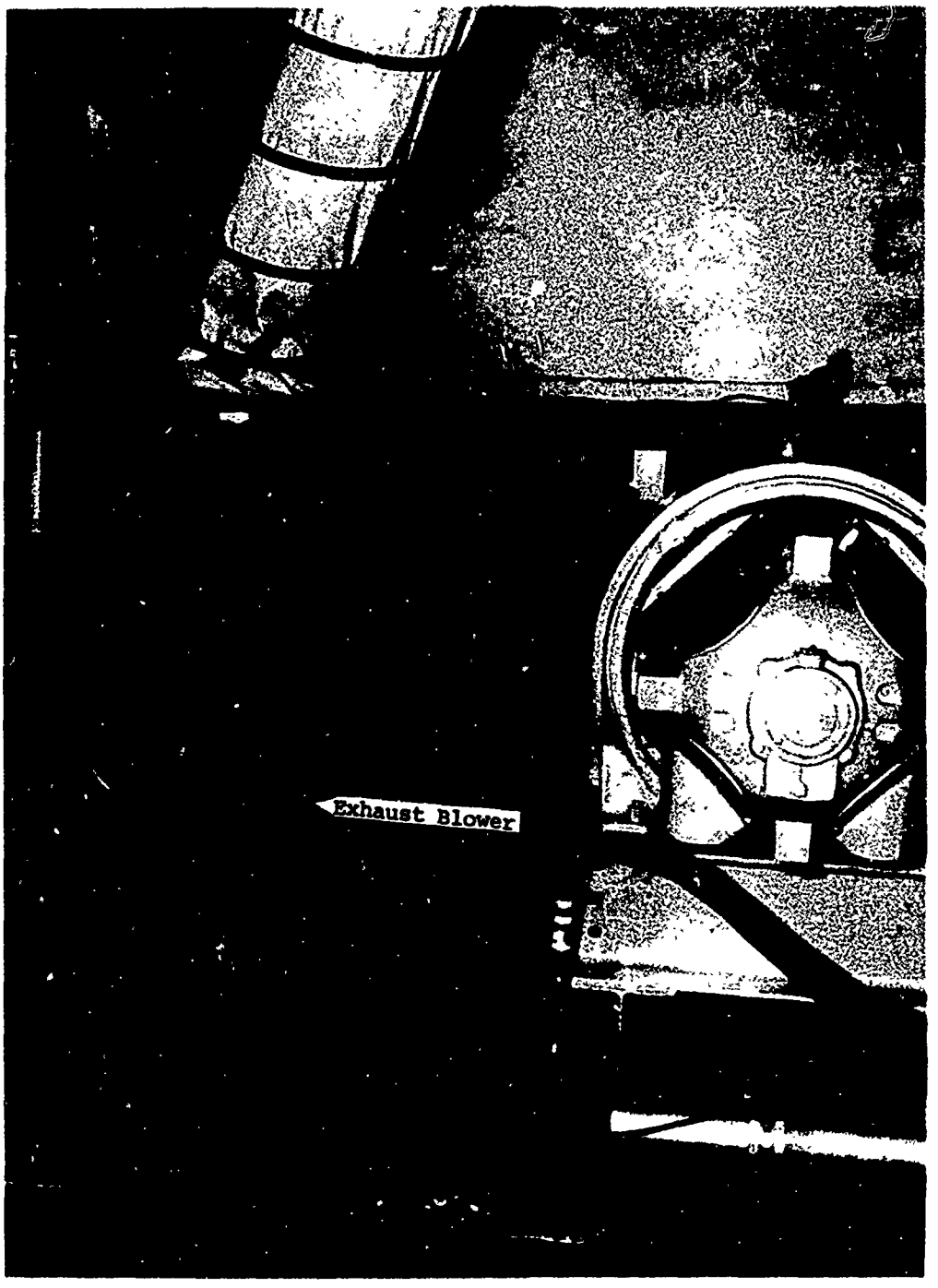

Figure 9. Test Chamber Air Exhaust Fan

SECTION III

DESIGN DEFINITION

1. DESIGN EVOLUTION

Preliminary considerations for defining facility design were directed toward creating a realistic compressor blade environment for material test specimens. One means of achieving this is to rotate the samples at a representative radius and tip speed while exposing them to a controlled environment of sand and dust. Several other rain and sand erosion facilities built on this principle have proved quite successful (see Bibliography). This approach permits high impact velocities to be obtained without requiring elaborate or costly hardware. For these reasons, the rotating arm approach was selected for the Air Force Aero Propulsion Laboratory's sand erosion facility.

Primary consideration was next given to the rotating arm and drive train layout. A sampling of turbine engines commonly exposed to sand and dust ingestion revealed that the average compressor is 30 inches in diameter; this was selected as the diameter of the rotating arm so that realistic centrifugal loads and material specimen sizes could be duplicated. A tip speed capability of 1400 ft/sec was originally selected as a representative level for advanced compressors, but this was later upgraded to 1600 ft/sec to comply with rapid increases in fan tip speed technology.

Once the arm diameter and speed was established, the detailed design of the arm began. Design goals were minimum stress and drag while maintaining a configuration that was simple to fabricate. The final design selected was a double taper arm with a diamond wedge cross section and 10% fineness ratio, as shown in Figure 10. The material specimens are attached to the arm tips with simple pins and snap rings for ease of removal.

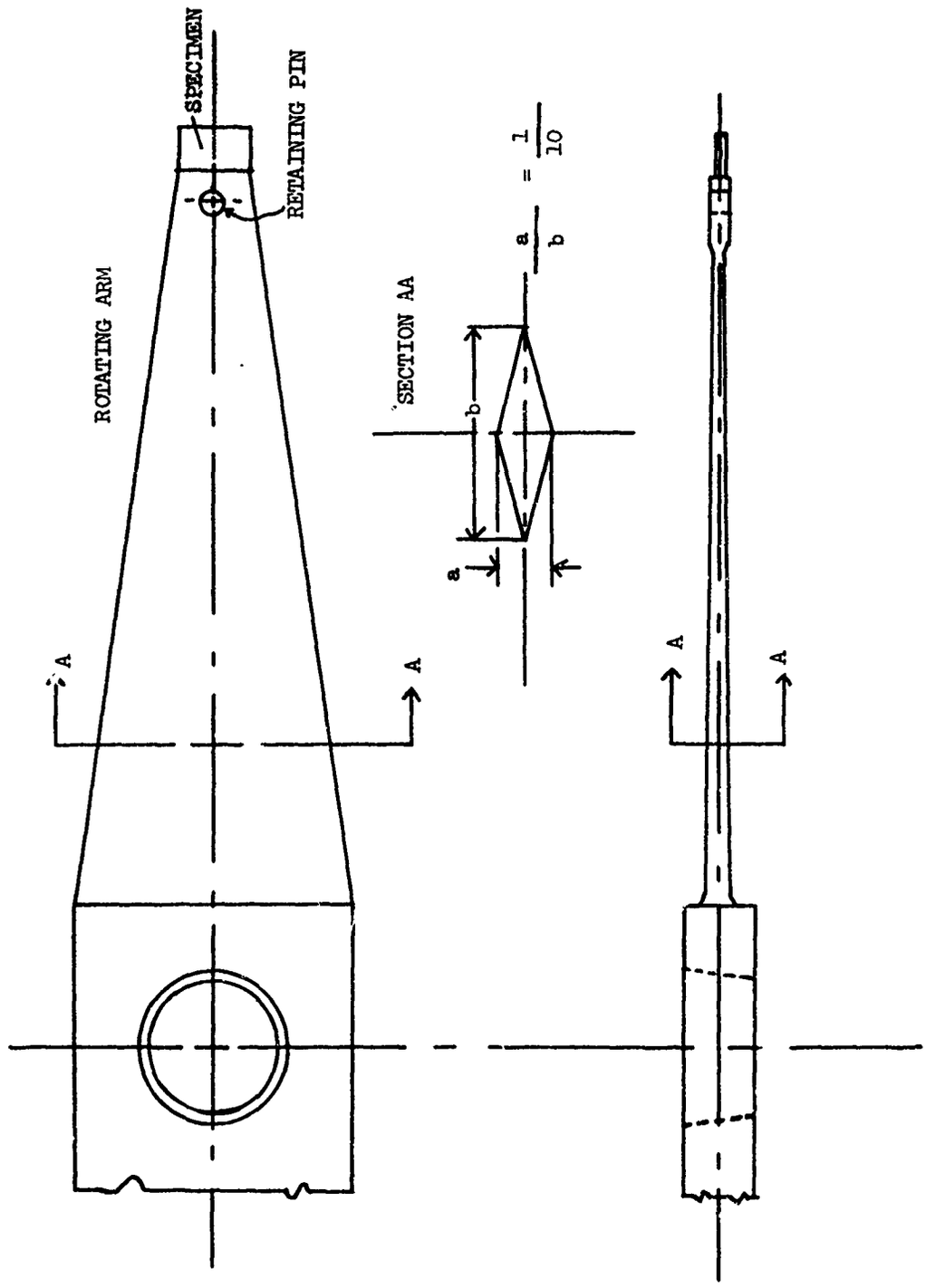

Figure 10. Rotating Arm Layout

To rotate the arm at 1600 ft/sec required about 100 HP. A 100-HP 3-phase AC variable-speed motor that was available in the laboratory was used. A speed-increasing gearbox was obtained to increase the output shaft speed from 3500 to 12,000 rpm. It was decided not to use the motor as a variable speed unit, but rather to employ a variable speed coupling between the motor and gearbox for speed control. That decision was made for several reasons: (1) the resistance bank needed for variable speed and the associated heat load could not be conveniently handled in the test cell; the variable speed coupling permitted a much simpler installation; (2) the coupling had a better speed controller than could be obtained from the motor; and (3) the coupling could be disengaged from the motor and used as a brake to stop the output shaft in emergencies. A later study conducted to investigate what was needed to increase the facility speed capabilities to 2000 ft/sec revealed that a direct-drive variable-speed DC motor and controller would be the simplest and least costly approach to upgrade the drive train. A vacuum shroud around the arm was considered to reduce power requirements but was abandoned as too complex and costly.

The original sand and dust control system for the facility consisted of a positive-displacement-type powder feeder, a 7-foot-long particle-acceleration nozzle, an exit duct, and a dry filter system. This arrangement was chosen for its simplicity and control of particle flow rate and velocity. The positive-displacement powder-feeder was chosen to control the flow rate, but proved to be unreliable because of the excessive wear caused by larger angular sand particles used in the test. To take the place of that unit, a simpler hopper and orifice arrangement was selected. Variable flow rates were then obtained by pressure control on the sand hopper and orifice diameter selection. The dry filter system was supplemented with a wet filter to contain the smaller sand and dust particles.

2. BLADE STRESS ANALYSIS

The blade shape, shown in Figure 10 has a double taper to the tip, and a diamond cross section with a 10% fineness ratio to achieve a

minimum stress and drag design. A simple steady state stress analysis was conducted for several materials to determine which would be most satisfactory. AISI 4340 alloy steel with a tensile strength of 170,000 psi was selected based upon its high strength and good erosion resistance. The maximum steady state stress on this material is about 47,000 psi at 12,000 rpm.

A dynamic stress analysis of the blade was conducted before the blade was run to its maximum tip speed to ensure that no critical operating ranges existed. The General Electric Company, Aircraft Engine Group, which was asked to aid in the dynamic analysis of the blade, provided a model of the blade, as shown in Figure 11, and analyzed it with their GE 635 Twisted Blade Card Program.

The results of the analysis, shown in Figures 12 through 17, indicated the design was sound, with the only critical operating range between 3000 and 6000 rpm. In that speed range, the 2/rev excitation frequency crosses the first flex mode, which causes high stresses. All other operating ranges appear safe for the first torsional modes. The effective steady state stresses for the leading, trailing, and maximum thickness edges were within 2% of each other and were plotted as one value in Figure 14. The Goodman Diagram for AISI 4340 alloy steel with 10^6 and 10^7 cycles runout (Figure 16) and the effective steady state stresses were used to obtain the allowable tip deflections for the first three fundamental modes, as shown in Figure 17.

In view of the analysis, no instrumentation, such as strain gages, was considered necessary to monitor the blade stress. The strobe light used to observe the test specimens could also be used to observe the maximum tip deflection during operation. Measured tip deflections for the first flex at speed can be compared with the allowable tip deflections in Figure 17 and a percent allowable stress determined. Similar stresses for second flex and first torsion can also be calculated from this figure.

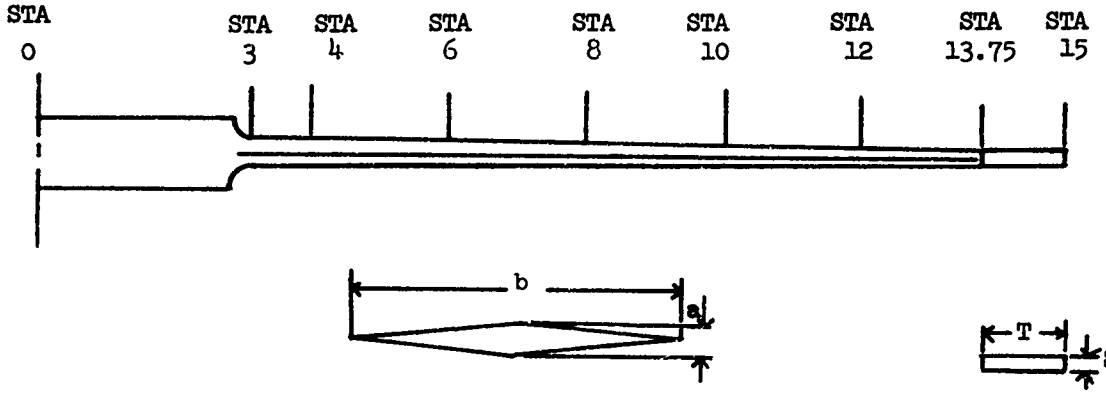

Dist. From Hub	a (in)	b (in)	Area (in^2)	I_x (in^4)	I_y (in^4)
3 in.	.485	4.85	1.17613	1.153 E-2	115.27 E-2
4	.455	4.55	1.03513	8.929 E-3	89.29 E-2
5.	.425	4.25	.903125	6.797 E-3	67.970 E-2
6	.395	3.95	.780125	5.072 E-3	50.716 E-2
7	.365	3.65	.666125	3.698 E-3	36.977 E-2
8	.335	3.35	.561125	2.624 E-3	26.238 E-2
9	.305	3.05	.465125	1.803 E-3	18.028 E-2
10	.275	2.75	.378125	1.191 E-3	11.915 E-2
11	.245	2.45	.300125	7.506 E-4	7.506 E-2
12	.215	2.15	.231125	4.451 E-4	4.452 E-2
13	.185	1.85	.171125	2.440 E-4	2.440 E-2
13.75	S =.25	T =1.625	.203125	5.290 E-4	2.235 E-2
15	S =.22	T =1.25	.1375	2.773 E-4	.8952 E-2

The analysis assumed that the arm was fixed at station 3 and had the shape of a homogeneous rectangular block between station 13.75 and 15.

Figure 11. Rotating Representation

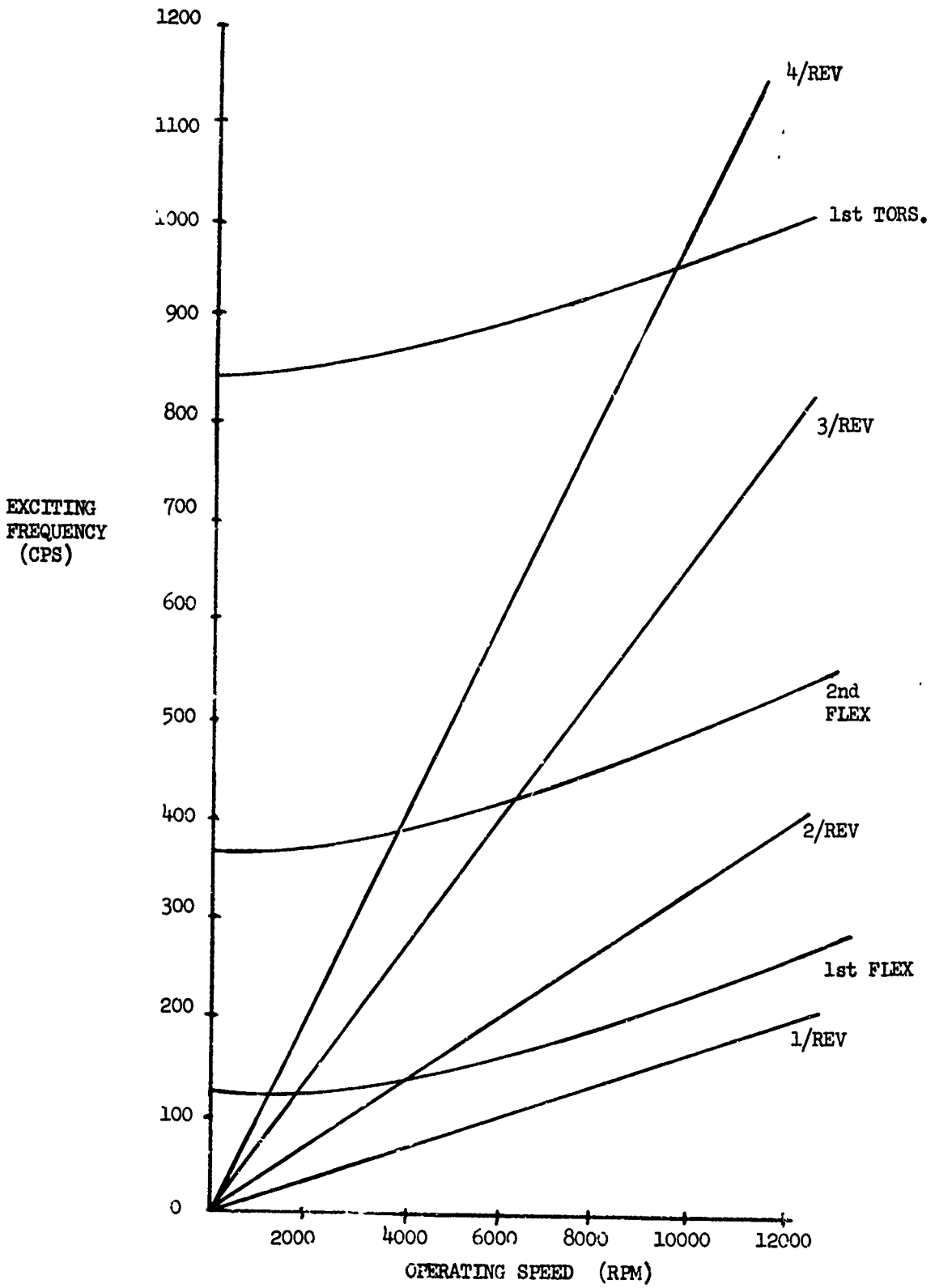

Figure 12. Campbell Diagram

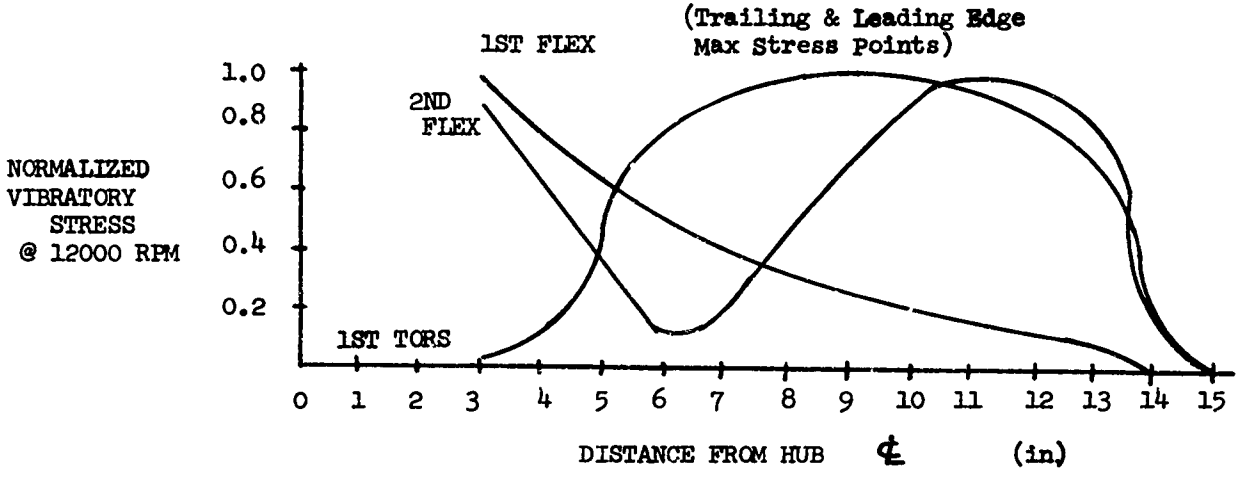

Figure 13. Rotating Arm Normal Stress

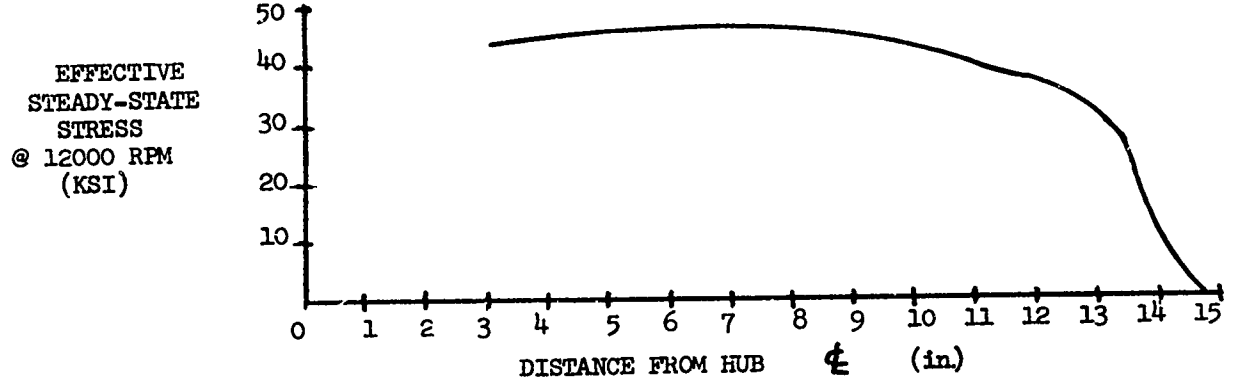

Figure 14. Rotating Arm Steady State Stress

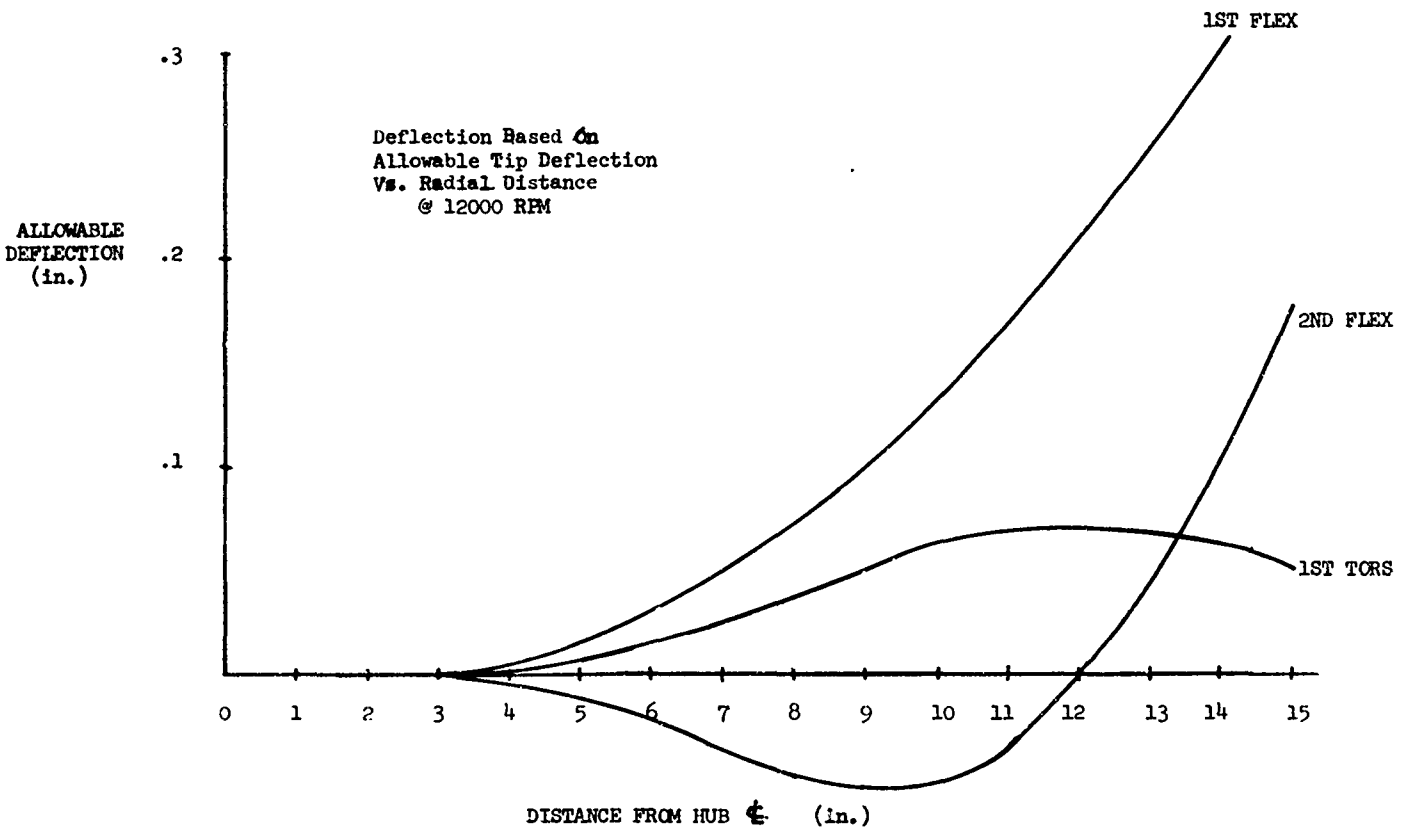

Figure 15. Rotating Arm Allowable Deflection

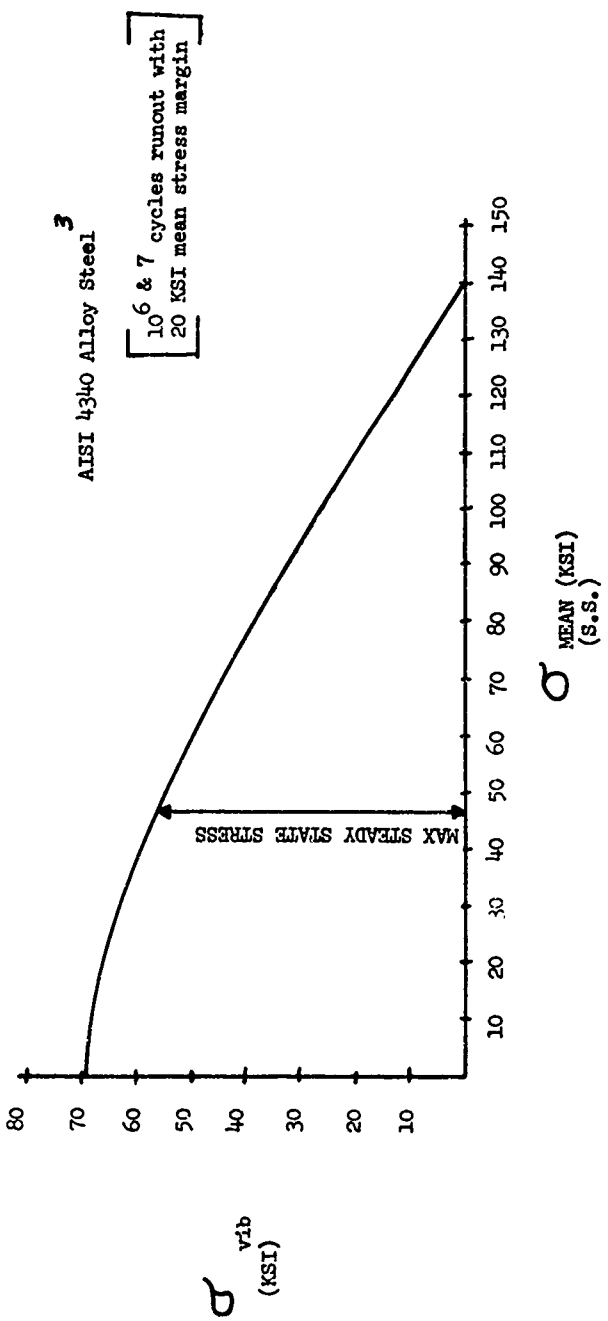

Figure 16. Goodman Diagram for Rotating Arm

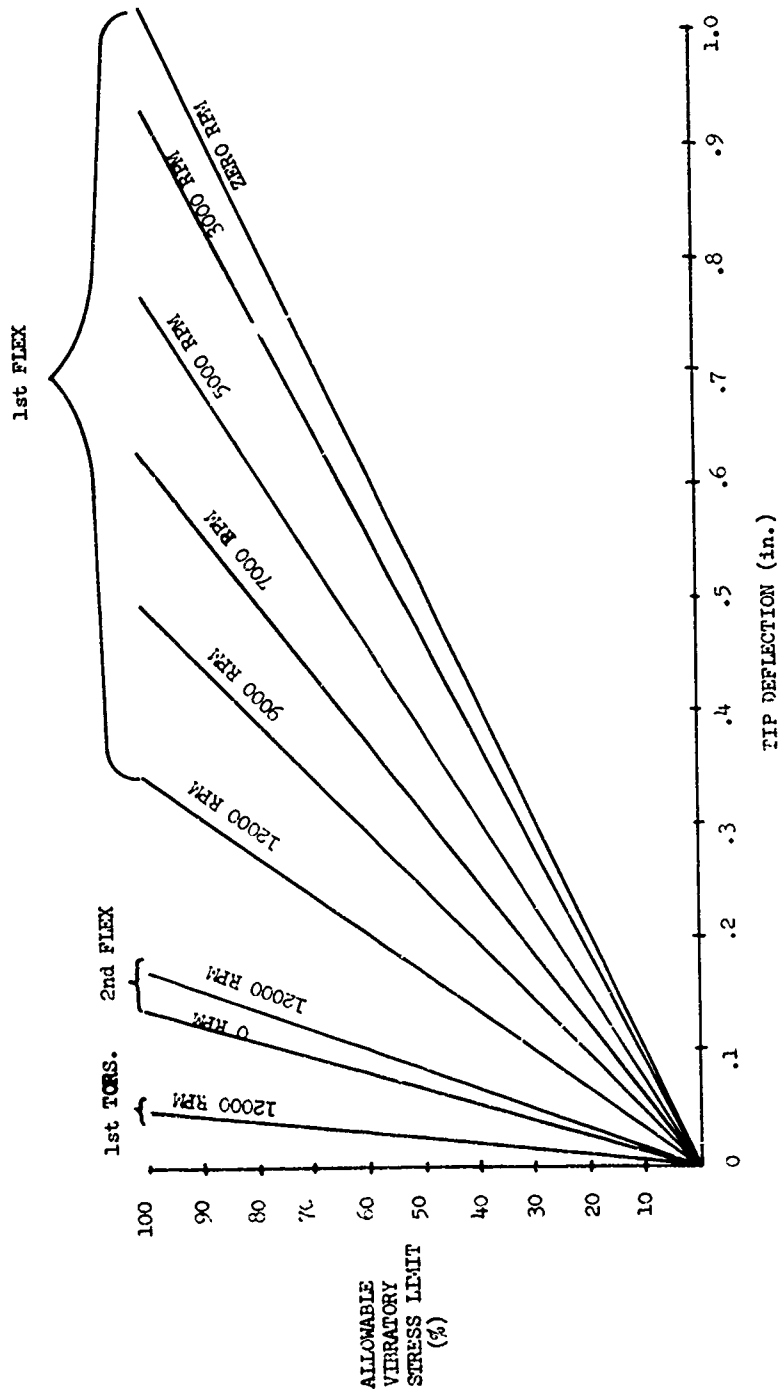

Figure 17. Stress Variation With Tip Deflection

3. BLADE POWER REQUIREMENTS

Once the geometry of the blade was defined, the power required to drive it at maximum speed could be calculated. This power requirement would then be used to size the drive train.

The analysis performed to determine the power required for the facility is presented in Appendix I. This analysis indicated that the system required 118 HP for a 1600 ft/sec blade tip speed. The 100 HP motor was used to drive the blade when the maximum tip speed was to be only 1400 ft/sec. Power readings on the 100 HP motor indicated that the power calculations were conservative, however; tip speeds of 1600 ft/sec have since been achieved with it.

4. DRIVE TRAIN

The established output shaft power and speed requirements set the drive train goals (i.e., 100 HP at 12,000 rpm). A counterwound variable speed induction motor rated at 100 HP was used to achieve these goals. Rather than operate the motor as a variable-speed unit, an adjustable-speed, eddy-current power coupling was added to the drive train for speed control. This unit was selected for its simplicity of installation, precise speed control, instant uncoupling, and output shaft braking. The last two qualities, uncoupling and braking, were considered necessary so that the rotating arm could be stopped in case of blade or sample failure. To complete the drive train, a gearbox was added to increase the motor output shaft speed from 3500 rpm to 12,000 rpm.

The motor is shut down automatically when oil pressure in the gearbox drops below a safe operating level or the cooling water is not circulated through the variable speed coupling. Other rig safety features include a start lockout prior to gearbox oil pressure and temperature being achieved, automatically activated warning lights, and horizontal and vertical vibration pickups mounted on the gearbox to sense vibration problems.

The drive motor, shown in Figure 18, is a Westinghouse variable speed unit. The variable speed coupling (Figure 19) is manufactured by Dynamatic Division of Eaton, Yale & Towne Inc. It is an adjustable-speed, eddy-current, slip device that transmits power by an electro-magnetic reaction between its driving and driven members. Accurate, sensitive control is achieved with a control system that varies the current in a single field coil. Output speed or output torque may be regulated (by using a control system which provides a wide range of stepless, adjustable speeds) to maintain a constant output speed (despite load changes) or a constant output torque. The gearbox, Figure 20, is manufactured by Western Gear Corporation. It is a high speed unit which features a pressurized oil system with water cooler.

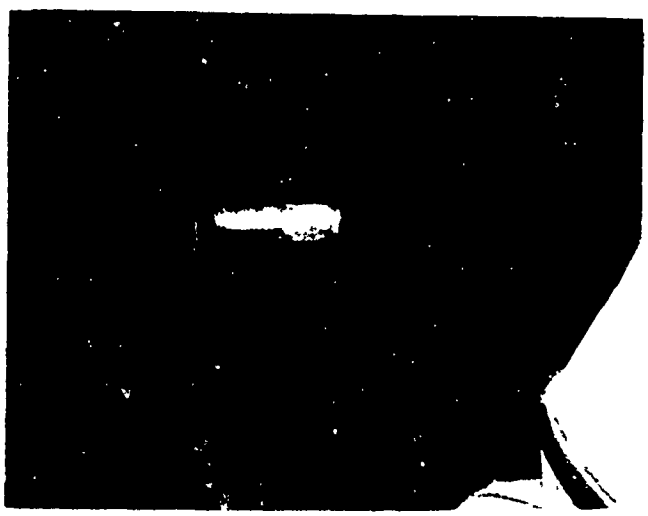

Type - CW Induction Motor
HP - 100
RPM - 3500
Voltage - 440 -3PH -60Cy
Amps - 118
Frame No. - 607-S

Figure 18. Drive Train Motor

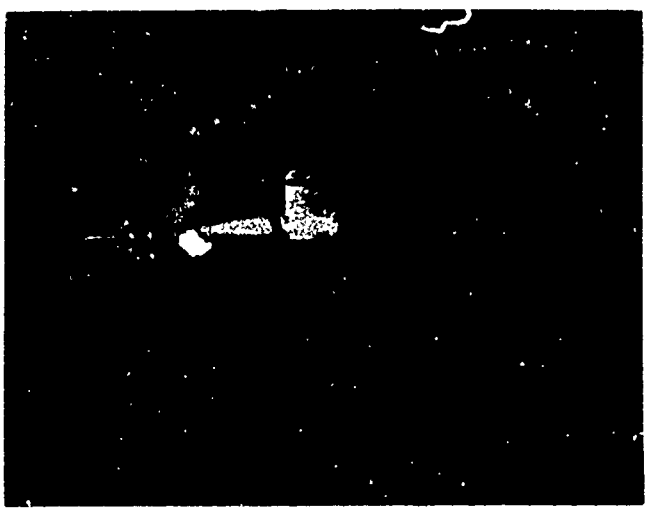

Model No.	- WCS 2103
HP	- 100
RPM	- 3500
Voltage	- 45 DC
Amps	- 6.4
Resistance	- 5.9 ohms
Coolant Water Pressure	- 35 psi
Control Input Voltage	- 230/460 AC

Figure 19. Variable Speed Coupling

Model No. - 4106
HP - 100
RPM IN - 3500
RPM OUT - 12,194
Ratio - 1:3.483
S. F. - 3.2

Figure 20. Drive Train Gear Box

5. SPECIMEN DESIGN

The sand erosion facility test specimen is designed to simulate tip sections of typical compressor blades. Blade tip sections are exposed to the most severe erosion environment by virtue of centrifugal effects and higher relative velocities. The centrifugal effects concentrate most of the ingested sand in the blade tip area and high tip velocities cause impact energies to be greater at the tip than on other parts of the blade.

A survey of turbine engine compressors revealed that a leading edge radius of 0.015 inch was representative of current design trends. With such a leading edge, a specimen thickness of 0.090 inch was considered ample to realistically model a typical compressor blade tip. To minimize material usage, but still obtain valid results, a test surface 3/4 inch long with a 1-1/4 inch chord was selected.

The current test specimen configuration is shown in Figure 21. Other geometries can readily be tested in this facility provided the specimen material strength is sufficient to carry the imposed stresses. Appendix II gives the minimum strength-to-density ratios which must be met by the test material for safe pin attachment to the rotating arm. The materials which are commonly used in compressor and fan blades meet these strength requirements. However, any of the advanced composite materials must be checked against the strength criteria.

6. CONTAMINANT CONTROL SYSTEM

To maintain the controlled environment required to investigate sand erosion parameters requires a sand feed and exhaust system which establishes flow at a uniform concentration and constant velocity. To provide this, a simple yet effective device was designed, as shown in Figures 6 and 7. The sand is held in a metal pressurized hopper and heated to prevent it from gaining moisture. Flow from the hopper is controlled by a calibrated orifice and a device to pinch the flow off. Once through the orifice, the sand falls into a seven-foot nozzle and is blown onto the rotating sample. The nozzle's seven-foot-length

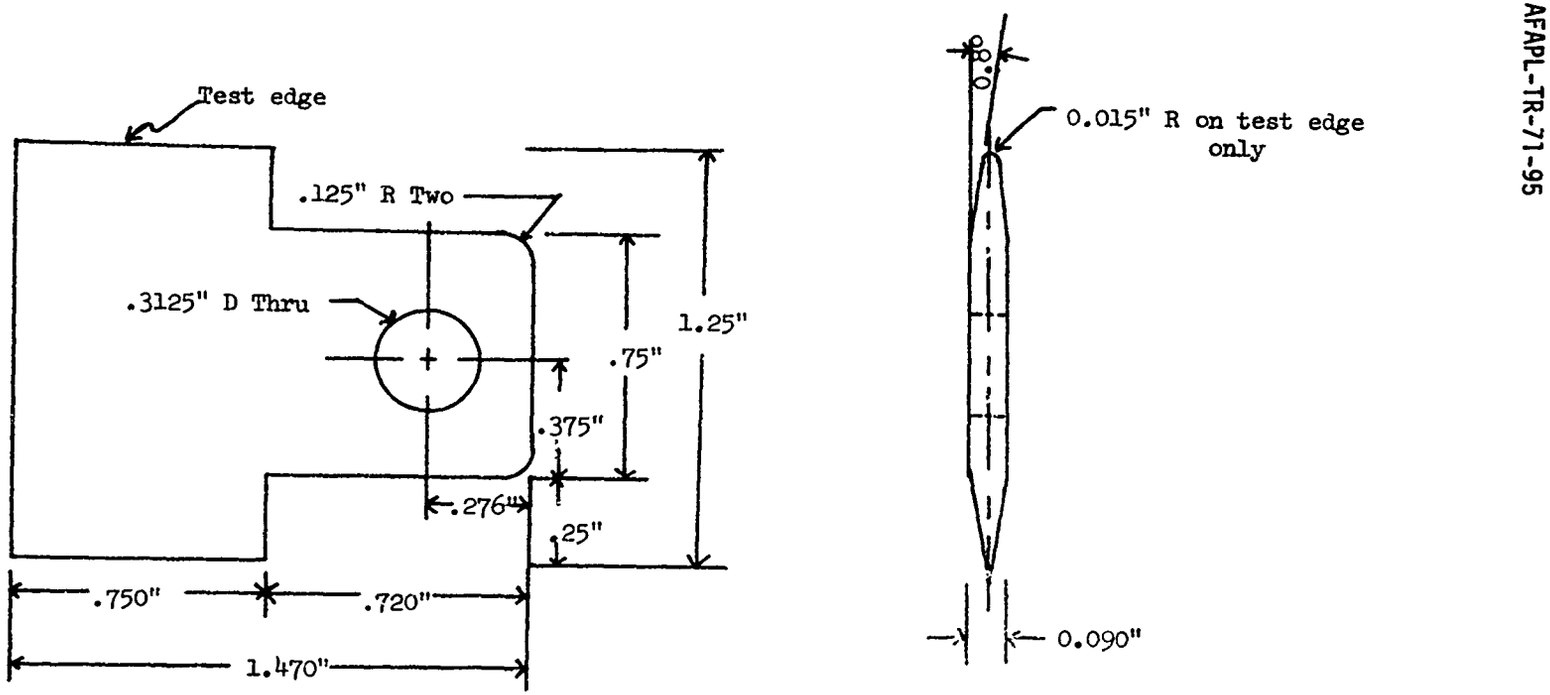

Figure 21. Test Specimen Configuration

establishes the sand flow. Air pressure for the nozzle is provided by standard 90 psi shop air passed through a filter and pressure regulator. Air velocity out the nozzle has been calibrated for a range of regulator settings, which is discussed in the calibration section.

The velocity of the sand exiting from the nozzle is assumed to be identical to that of the exiting air. This is only an approximation, of course; when more precise values of this velocity are needed, a more exact measuring system will be devised. Exact measurements are important for studies of impact angle effect, but are of small significance to the total relative impact velocity. Present studies are directed toward relating impact velocity to erosion rate.

Once the sand passes through the sample arc, it is exhausted into a 4-inch diameter tube, which leads out of the test chamber and into an expansion box where the larger sand particles can settle out. Air from this box then passes through both dry and wet filters in an attempt to capture the remaining fine sand particles. A small exhaust fan aids in moving the air through the settling box and filters. This exhaust system has proven very effective in that only small amounts of sand have been found in the test chamber after a run and little sand passes completely through the filter system.

A schematic of the complete contaminant control system is shown in Figure 22. Test samples run with this system indicate that the desired erosion pattern is being achieved. The reproducibility of test results indicates that the tests are being accomplished in a consistent manner.

7. TELEVISION MONITOR

A method of observing the samples during a test was considered necessary from both the data acquisition and the safety viewpoints. Visual records of sample erosion are useful in determining when the maximum erosion rate occurs or how a particular blade coating or leading edge protection fails. From the safety aspect, the loss of a test sample or excessive blade tip deflection can be observed to warn of conditions requiring rig shut down.

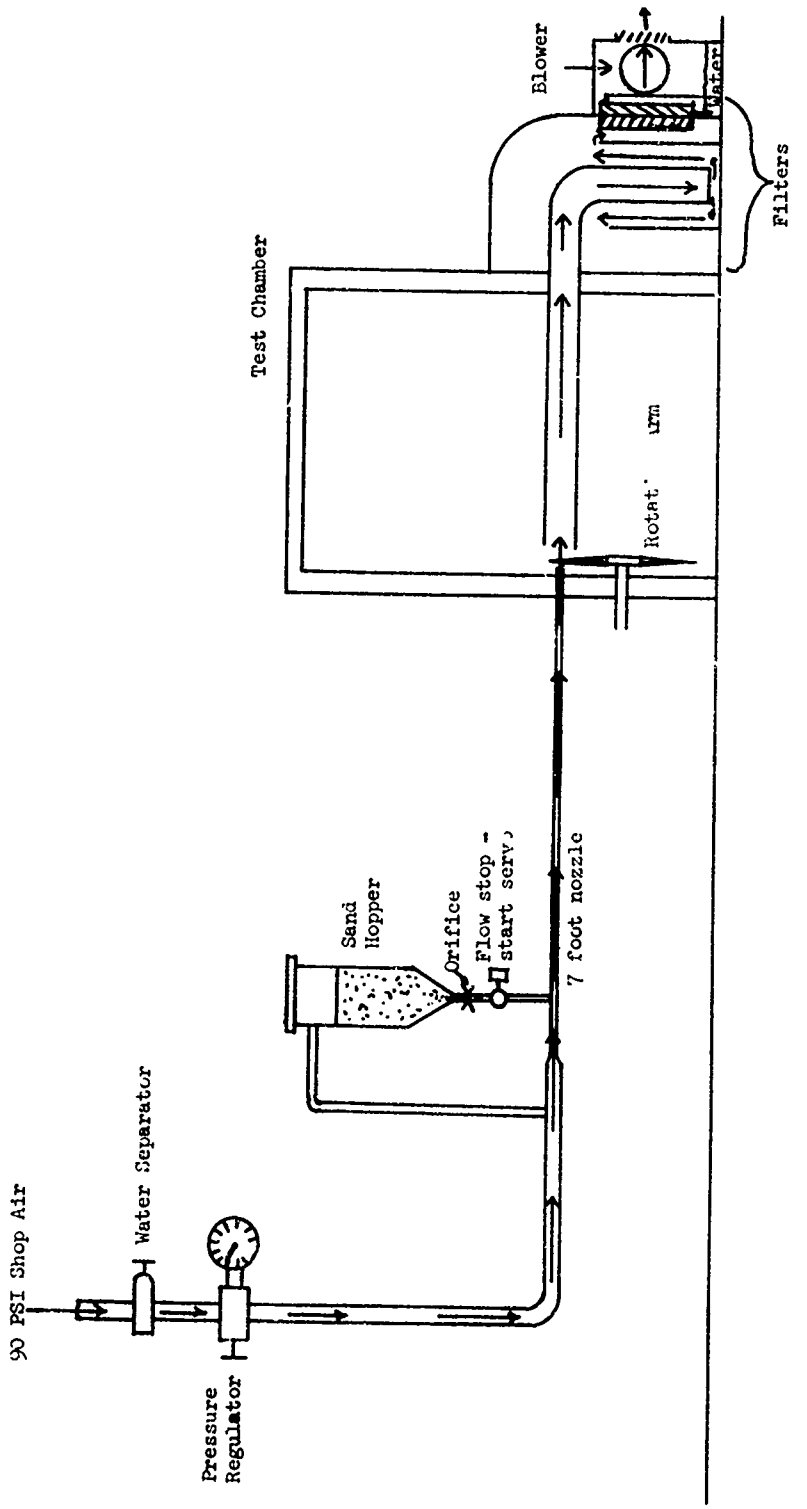

Figure 22. Contaminant Control System Schematic

Periscope or television monitors had been used on previous erosion facilities to observe test operations from the safety of the control room. The periscope has the advantage of high resolution, but it is only practical over short distances. Television is easy to install and is insensitive to distance, but lacks high resolution.

Since the necessary television equipment was available in the laboratory, we decided to use it in an early test run. The results were satisfactory, so the system was permanently installed. The resolution is adequate to observe large particle impacts and leading edge geometry changes.

We also installed a stroboscopic system for observing the tests. Figure 4 shows this installation along with the television camera. A window cut in the test chamber wall allows the strobe light and television camera to focus on the test specimen. The strobe was originally triggered by a photoelectric pickup, which responded to a reflective tape mounted on the output shaft. On high-speed runs, however, small amounts of oil from the shaft bearing would coat the tape and the photoelectric pickup lens and render the system inoperative. A 60-tooth gear and magnetic pickup had also been mounted on the output shaft for RPM monitoring. The magnetic pickup signal was modified to trigger the strobe, replacing the photoelectric trigger. This new system has proven completely satisfactory. A flash delay has been included in the strobe circuit so that either of the test specimens can be brought into the camera viewing field by a simple adjustment. The schematic for the strobe and television circuits is shown in Figure 23.

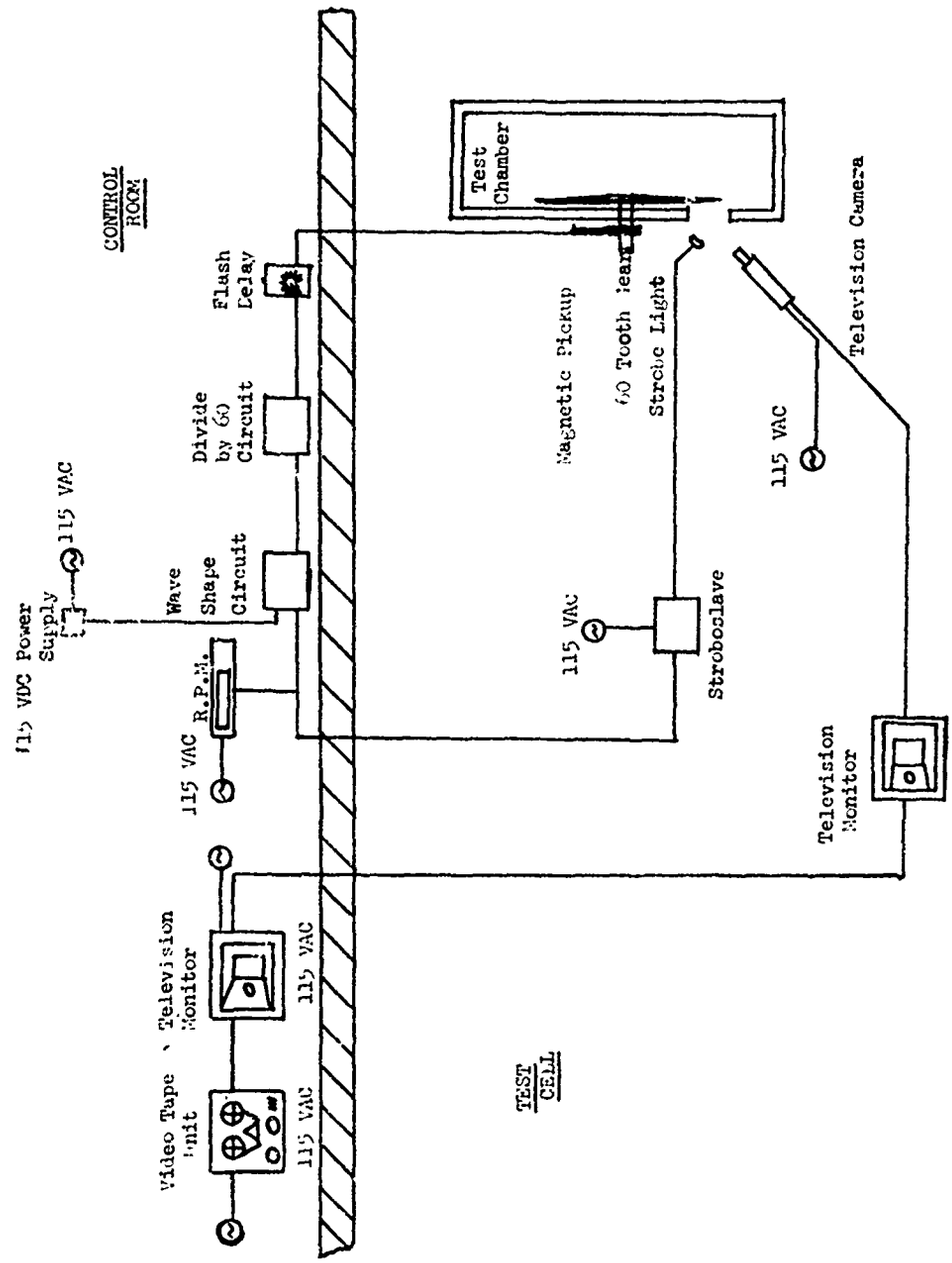

Figure 23. Television Monitor Schematic

SECTION IV

CALIBRATION EXPERIMENTS

1. SAND FLOW RATE

The sand flow rate from the hopper is controlled by a simple orifice. Flow through the orifice is a function of the pressure drop across the orifice, sand particle size, and sand wetness. To minimize the effect of wetness, the sand in the hopper is kept dry with a heat lamp. Also, the sand particle size distribution is held as constant as possible. This should allow the sand flow to be calibrated as a function of nozzle pressure, which is directly related to the orifice pressure drop.

The calibration was accomplished by timing a known weight of dry sand through the orifice at a given nozzle pressure. One and two pounds of MIL-Spec distribution sand were timed at pressures between ten and thirty inches of mercury. The results have been plotted in Figure 24.

The ±5% error obtained can most likely be attributed to the large variation in size of the MIL-Spec sand particles and to the small orifice, which was only slightly larger in diameter than the largest sand particle. However, the flow rate of sand only determines the concentration per unit time to which the test specimens are exposed. Total specimen exposure is determined by the amount of sand loaded into the hopper. Previous experiments have indicated that slight changes in sand concentration do not affect the specimen weight loss as long as the total amount to which the specimen is exposed is held constant. Therefore, the orifice calibration is only important for determining the approximate test run time for a given sand exposure, and in no way affects the quality of the test. For this reason, no attempt was made to determine the flow rate more precisely.

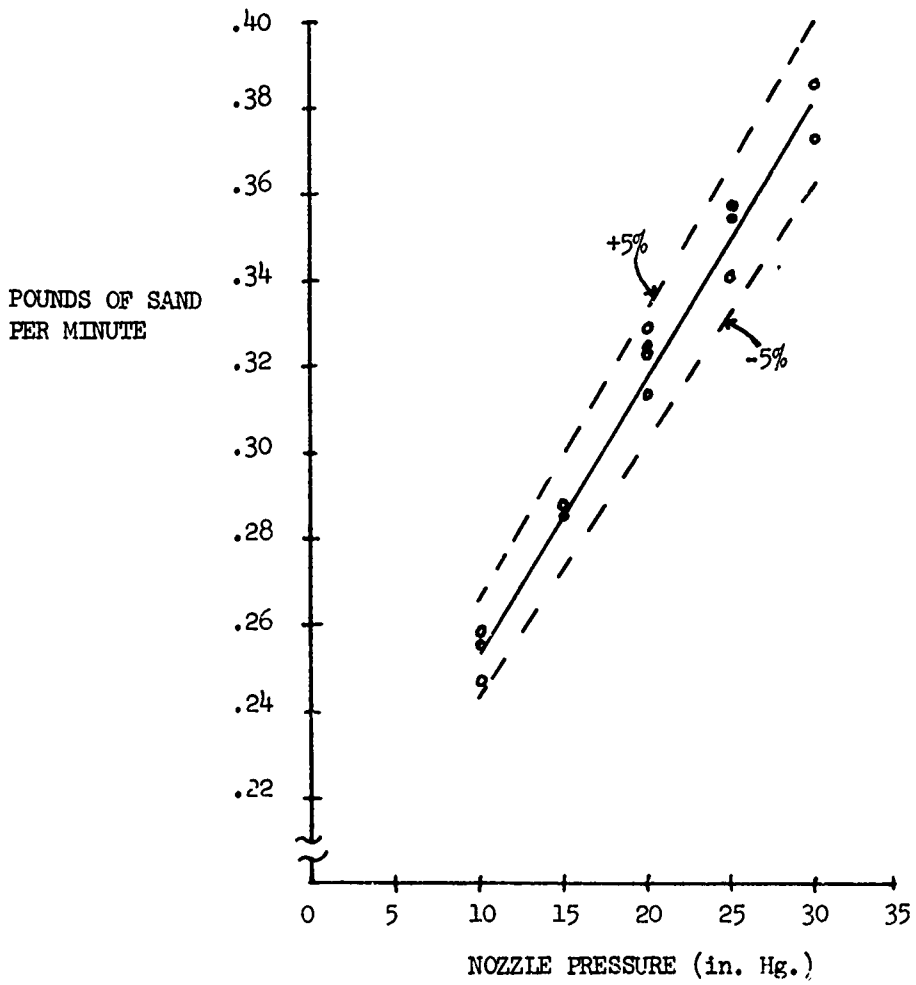

Figure 24. Sand Flow Calibration

Of equal importance with the sand flow rate is the percent of sand which hits the specimen. If the specimens were infinitesimally thin, the ratio of specimen area to arc area swept by the specimen would equal the percentage of sand which actually hit the specimen. However, the specimens have a 0.090" thickness, so their projected area ratio increases as the impact angle decreases. This phenomenon is illustrated in Figure 25.

A plot of the projected area ratio for various impingement angles is shown in Figure 26. The projected area is assumed equal to the percent of sand impacting the specimen. An important point to note is that the percent of sand impacting the specimen remains constant for a given impingement angle, regardless of the specimen speed.

2. SAND VELOCITY

The true sand particle velocity is an important parameter in erosion experiments with this facility, since it is directly related to the relative impact with the test specimen and the energy associated with that impact. Both the impact angle and energy are critical quantities affecting erosion rate. The sand velocity was assumed to be equal to the air velocity leaving the sand blast nozzle. This nozzle was specifically designed with sufficient length to allow the sand particles time for accelerating to the air velocity before impacting the samples. The nozzle exit air velocity was measured with a pitot tube and a mercury manometer. This velocity was then plotted versus nozzle pressure and is shown in Figure 27.

3. MATERIAL BASELINE

The baseline calibration of the facility has not been completed but we have included here typical test procedures and initial results. At this time, only three materials have been tested on the facility: 6061 Aluminum, 6-4 Titanium, and INCO 718. Other typical compressor blade materials to be included in the baseline are various steels, titaniums, and unprotected composites, such as boron/aluminum and graphite/epoxy. Data from the material baselines will be compared with that obtained from other erosion facilities and from service engine experience to establish

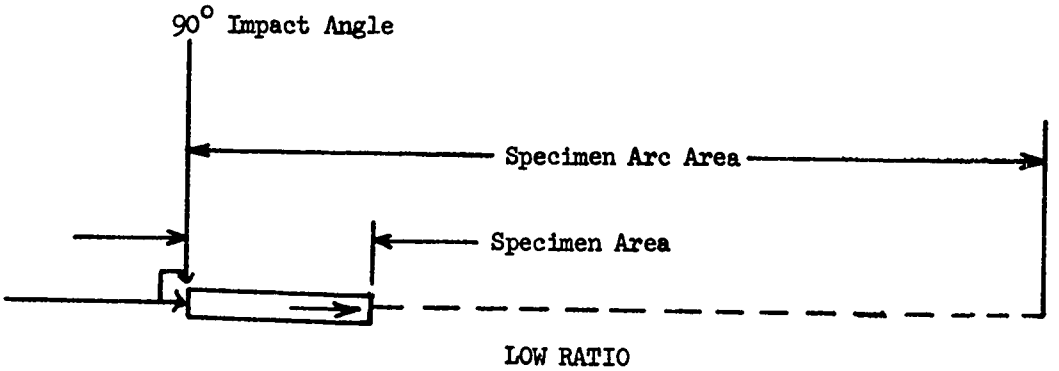

LOW RATIO

$$\text{RATIO} = \frac{\text{Specimen Area}}{\text{Specimen Arc Area}}$$

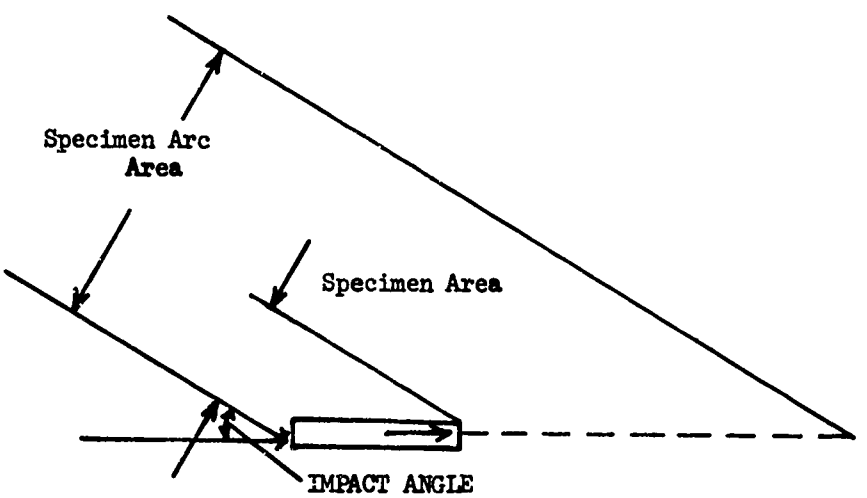

HIGH RATIO

Figure 25. Effect of Impact Angle on Exposure Area

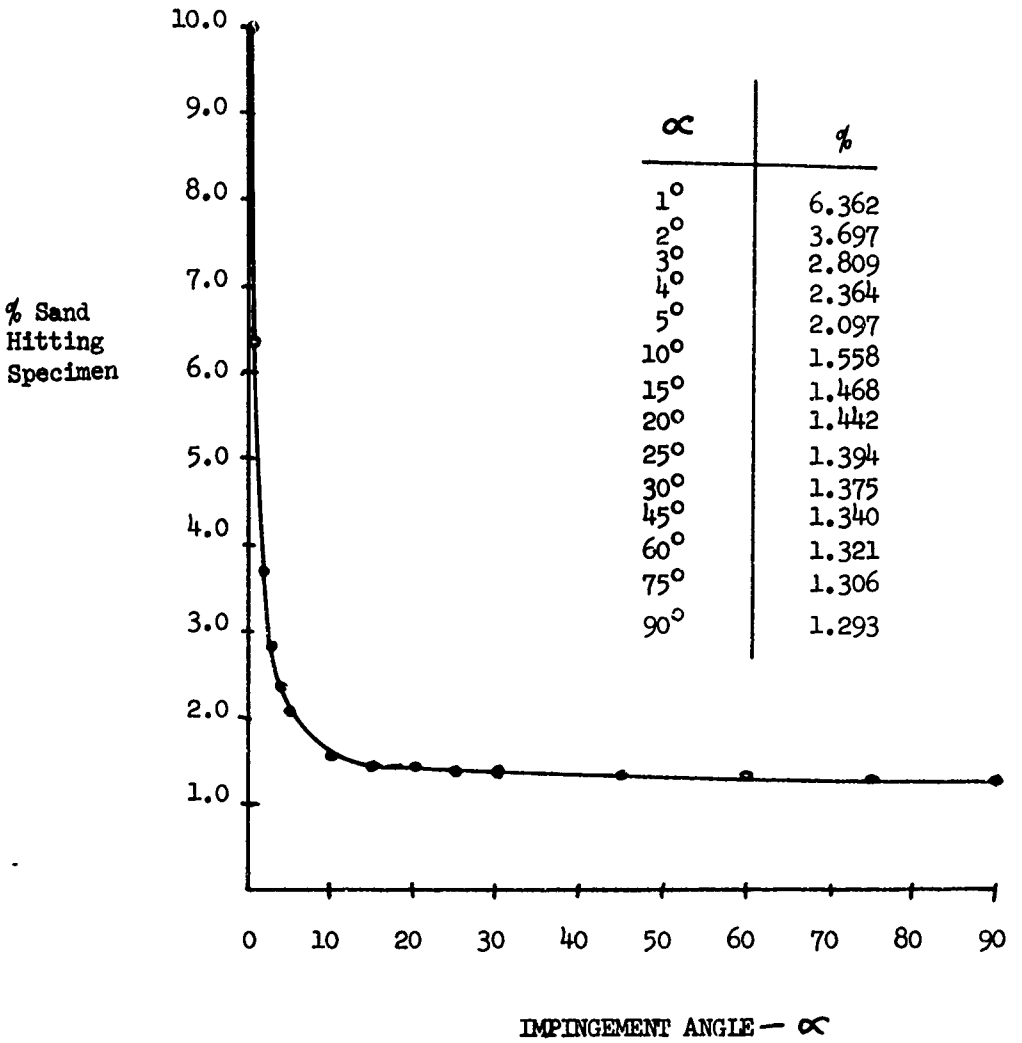

∝	%
1°	6.362
2°	3.697
3°	2.809
4°	2.364
5°	2.097
10°	1.558
15°	1.468
20°	1.442
25°	1.394
30°	1.375
45°	1.340
60°	1.321
75°	1.306
90°	1.293

Figure 26. Sand Exposure Variation With Impact Angle

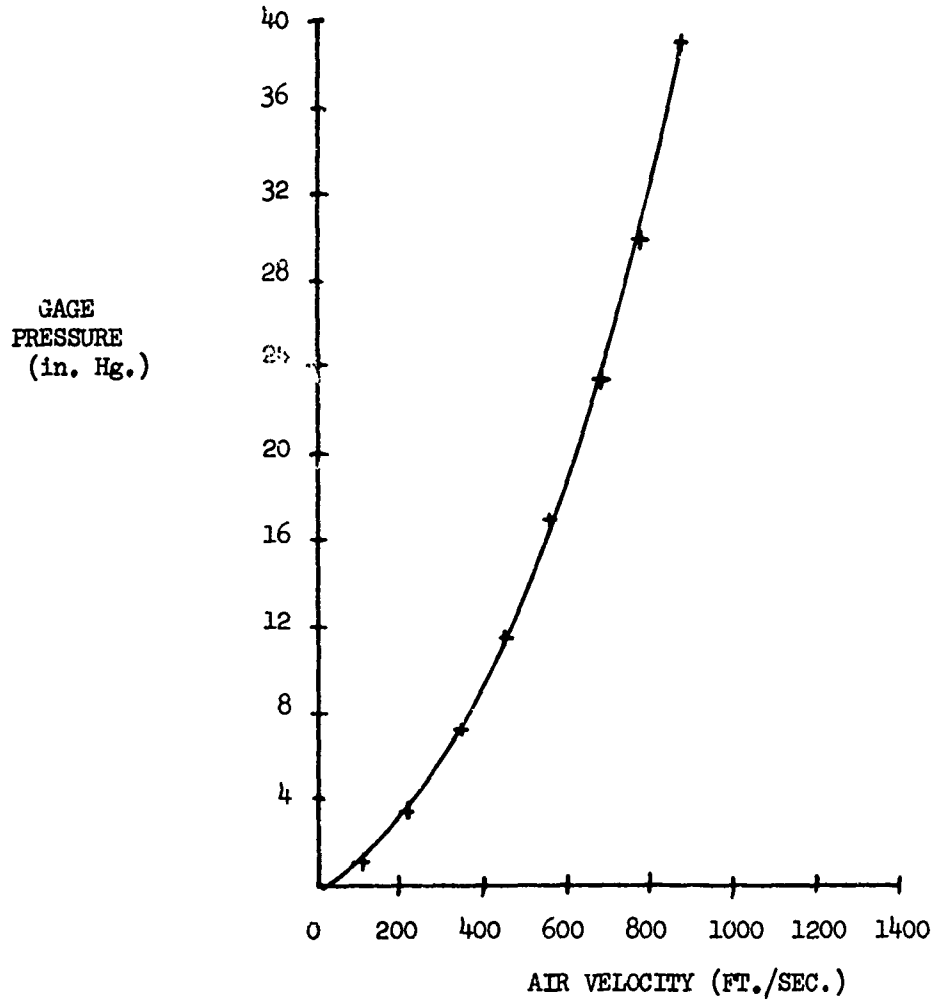

Figure 27. Air Velocity Calibration

the validity of the baseline test results. Then the data will be used to evaluate other materials, coatings, protection schemes, and specimen geometries on a relative basis.

The initial test matrix was established with the goal of using a minimum number of specimens to obtain the baseline data. As many as six variable parameters could have been chosen for the test matrix; however, only specimen material and impact velocity were selected as the required minimum. Specimen geometry, impact angle, sand quality, and sand quantity are the remaining variables, but they either have little effect on the relative ranking of materials or they tend to remain nearly constant in an actual engine. The specimen geometry was made representative of a "state-of-the-art" compressor blade leading edge. An impact angle of 25° was selected because it is near the maximum impact erosion angle for ductal materials and at the same time within a realistic range for an actual engine. The maximum erosion impact angle had been previously determined by various experimenters to be about 30°. Sand quality was established by the military specification and quantity was set to achieve an approximately 1% weight loss as a desired level of erosion on the specimens. Once the material selection was completed, only the impact velocity schedule was needed to complete the test matrix. The impact velocity is a function of both specimen velocity and sand velocity, as can be seen in Figure 28. The specimen velocities were selected to cover speeds ranging from those obtained previously in low speed facilities, to the maximum capable in the new facility -- 733, 880, 1100, 1400, and 1600 ft/sec. The sand velocity was next selected to maintain a constant impact angle of 25°. The complete test matrix is shown in Table I.

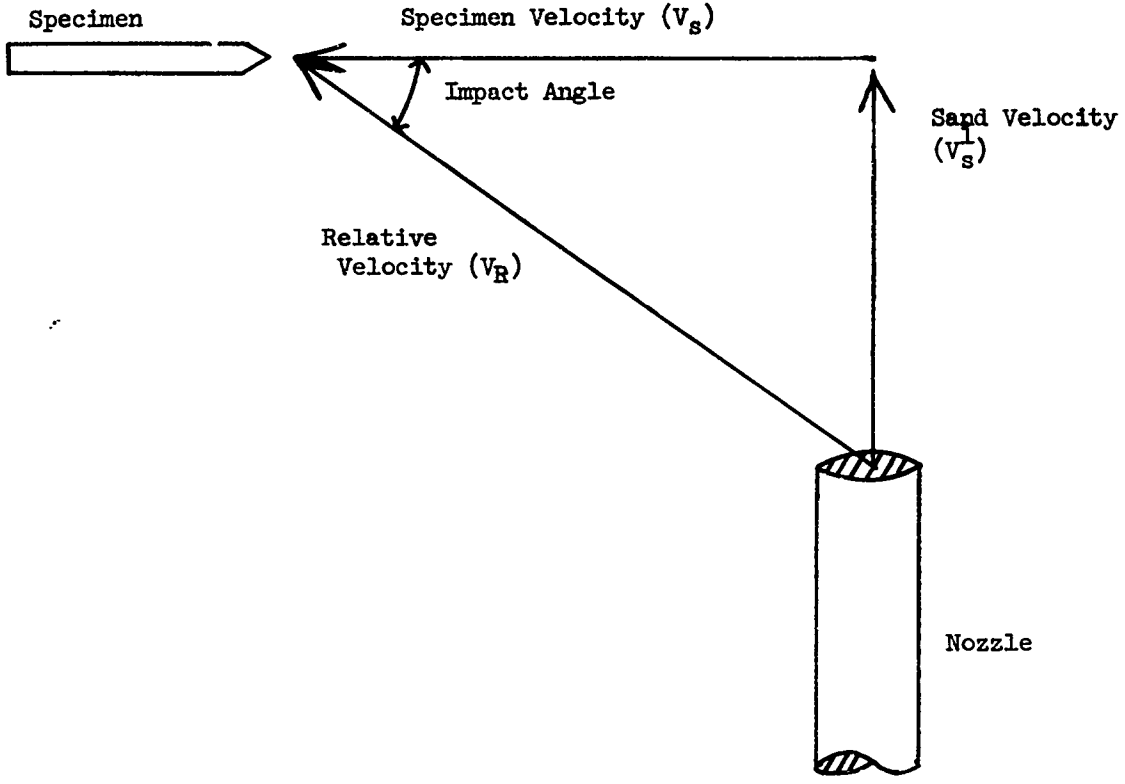

$$V_R = \sqrt{V_s^2 + (V^1_s)^2}$$

Figure 28. Particle Impact Velocity Triangle

TABLE I

INITIAL SAND EROSION FACILITY TEST MATRIX

Specimen Material----------Aluminum, Titanium, Inco
Specimen Geometry----------0.015" leading edge
Sand Quality ----------Mil Spec
Sand Quantity ----------two pounds
Impact Angle ----------25°

Tip Speed ft/sec	Rotational Speed RPM	Sand Speed ft/sec	Relative Velocity ft/sec
733	5333	342	809
880	6403	410	971
1100	8003	513	1214
1400	10186	653	1545
1600	11644	746	1765

Table II contains the initial test results expressed as both weight and volume loss. A log - log plot of volume loss versus relative velocity has been made in Figure 29. A slope of two was obtained with the Inco 718 specimens; the titanium and aluminum slopes are slightly higher. The slope of two indicates that the volume loss is proportional to the kinetic energy of the particle impact. The greater slopes for the titanium and aluminum materials are difficult to explain, but they may be related to the lower melting temperatures of these materials. Figures 30, 31, and 32 show the relative degree of damage between the three materials at 733, 1100, and 1600 feet per second tip speeds.

TABLE II

INITIAL TEST RESULTS

MATERIAL	RELATIVE VELOCITY (ft/sec)	WEIGHT LOSS* (grams)	VOLUME LOSS* (cm^3)
Aluminum 6061	809	.0467	.0174
	971	.0775	.0289
	1214	.1370	.0512 **
	1545	.2725	.1017
	1765	.4180	.1568
Titanium 6-4	809	.0389	.0088 **
	971		
	1214	.0890	.0197 **
	1545		
	1765	.2064	.0459 **
INCO 718	809	.0857	.0104
	971	.1205	.0148
	1214	.1631	.0199 **
	1545	.2521	.0345
	1765	.3292	.0400 **

*Average of two specimens

**Average of two test runs (reproducibility check)

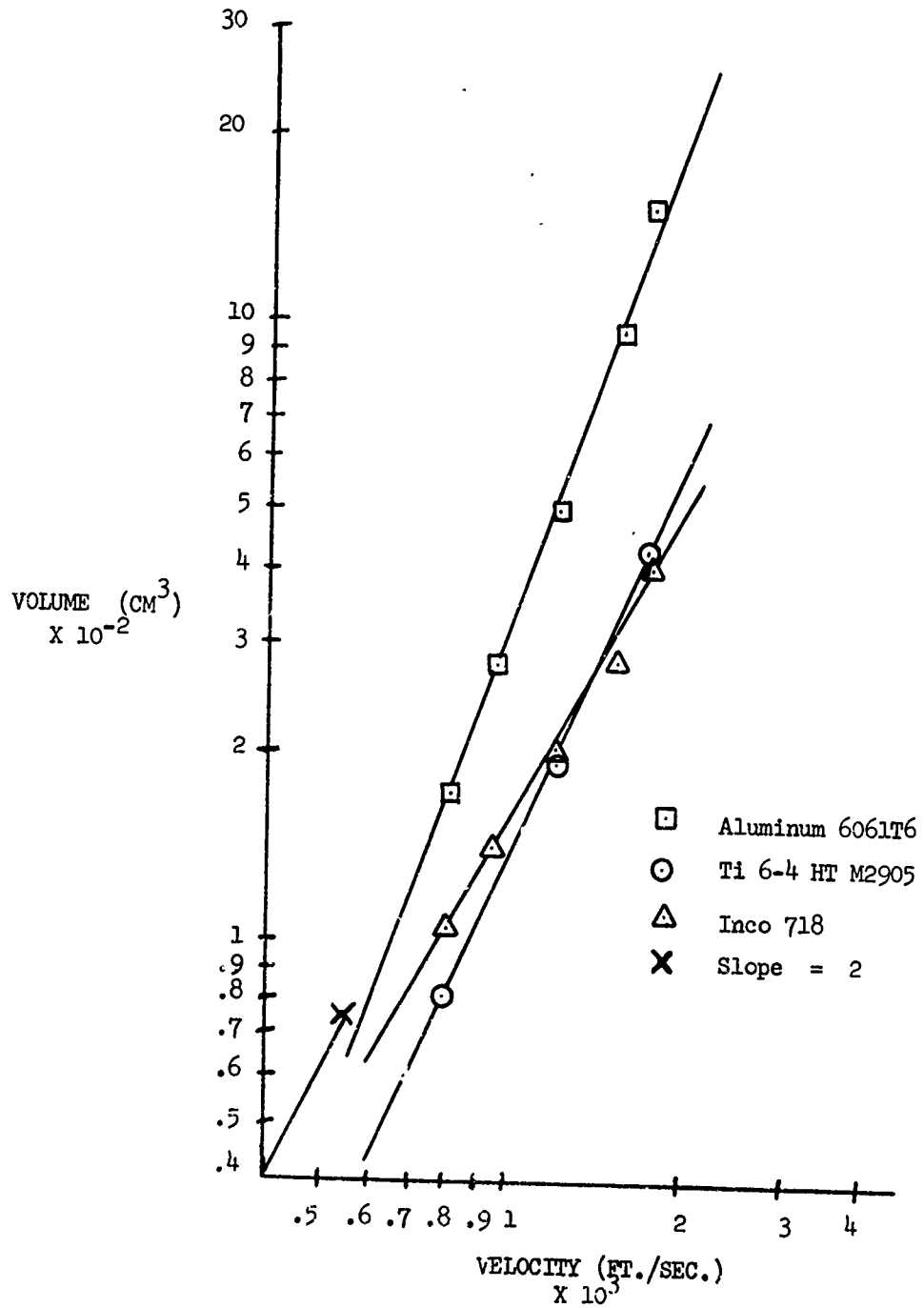

Figure 29. Erosion Correlation With Particle Impact Velocity

Figure 30. Inco 718 Specimens

Figure 31. 6061 Aluminum Specimens

Figure 32. 6-4 Titanium Specimens

SECTION V

DISCUSSION OF RESULTS

Thirteen test conditions have been evaluated as of the writing of this report. For a reproducibility check, 6 of the test conditions were run twice, for a total of 19 data points. At each data point checked for reproducibility, the results were within experimental error, indicating that the facility gave good reproducibility. Sufficient data has not been generated to allow correlation with other facilities, but the initial tests do allow a reasonable facility assessment. In general, the facility has proven quite satisfactory and reliable. On the average only 20 minutes are needed to test a set of two specimens. This time includes mounting the specimens, loading the sand hopper, running the erosion test, and removing and weighing the specimens. All the features of the facility combine to allow inexpensive, quick, and reliable material evaluation and parameter investigation.

The only weak point of the facility appears to be in the rotating arm design. After many hours of facility checkout, two troublesome areas in the arm design have been identified. Despite precautions, some sand does hit the arm and causes significant erosion -- enough, in fact, that the arm has to be replaced after about 50 hours of high speed testing. A better arm design would incorporate a thicker leading edge for better erosion resistance or low cost replaceable tips. In addition, the specimen attachment design should be modified. The present attachment method is simple and works well for most materials, but it requires the material to have a higher shear strength than some composites have. The attachment design should take into consideration all materials to be investigated.

As was previously mentioned in this report, a study was made to determine what steps were necessary to increase the tip speed capability of the facility. The results of that study indicated that a 200 HP variable speed DC motor and power supply would be the least expensive approach for a 2200 ft/sec facility. A DC motor would be simpler to

install and maintain than the three unit drive train used in the present facility, and no safety or control features would be sacrificed. If a facility is to be planned and no available motor or other drive train component can be used, then the DC motor unit appears to be an attractive approach.

SECTION VI

CONCLUSIONS

1. A rotating arm apparatus has been constructed at WPAFB, Ohio and is operational; this device is capable of sand erosion simulation at specimen velocities up to 1600 ft/sec.

2. The apparatus has demonstrated consistency and reproducibility in its operation.

3. The goal of low-cost-per-unit specimen, high-speed erosion testing has been achieved.

SECTION VII

FUTURE PLANS

1. Research on the rotating arm apparatus will continue to investigate the erosion behavior of current and new compressor blade materials at velocities up to 1600 ft/sec.

2. High speed photography will be used to calibrate the sand particle velocity.

3. Effects of environmental variables such as velocity, impingement angle, sand particle size, and sand concentration will be investigated.

4. Effects of material variables such as leading edge radius, coating thickness, and composite construction techniques will be investigated.

APPENDIX I

BLADE POWER REQUIREMENT

The blade drag and rotating speed determine the power required. Since the blade drag is a function of its chord, a relationship between the chord and the blade radius would be useful. Because the blade has a constant taper, the relationship between chord and radius is linear and can be expressed as follows (Reference 4):

$$c = c_B \left[1 - \frac{(m - 1)}{m} \frac{r}{R} \right] \qquad (1)$$

Where $m = \frac{c_B}{c_T}$

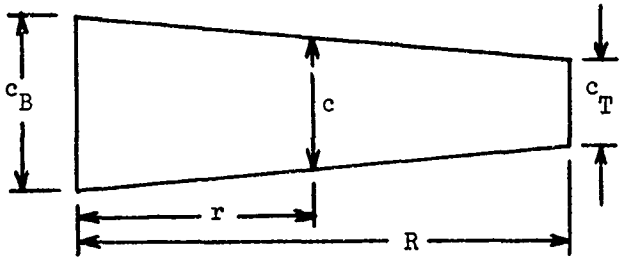

An approximation of the blade drag (C_D) variation with Mach number (M) for a 10% fineness ratio is expressed as follows (Reference 4):

$$C_D = \frac{\cdot\cdot}{10} \qquad 0 < M \leq 1$$

$$C_D = \frac{1}{10M} \qquad 1 < M \leq M_{tip}$$

With expressions for the blade chord and drag coefficient defined, the torque required to turn the blade can be expressed as follows:

$$\text{Torque} = \int \frac{1}{2} \rho \, C_D V^2 \, c \, r \, dr \qquad (2)$$

where ρ = air density
V = velocity at radius r
w = rotational speed of arm

$$r = \frac{V}{w} \qquad dr = \frac{dV}{w} \qquad w = \frac{V_{tip}}{R}$$

$$\text{Torque} = \int \frac{1}{2} \rho \, C_D V^2 \, c \, \frac{V}{w} \, \frac{dV}{w} \qquad (3)$$

$$\text{Torque} = \frac{\rho}{2w^2} \int C_D \, c \, V^3 dV \qquad (4)$$

$$\text{Horsepower} \quad HP = \frac{(\text{Torque})\,(w)}{550} \qquad (5)$$

$$\text{HP required} = \frac{\rho}{1100w} \int C_D c \, V^3 dV \qquad (6)$$

Substituting Equation (1) for c and letting V = 1100M, one obtains from Equation (6)

$$HP = \frac{\rho R}{(1100) M_{tip}} \int C_D c_B \left[1 - \frac{(m-1)}{m} \frac{1100 MR}{1100 M_{tip} R} \right] (1100M)^3 dM \qquad (7)$$

$$HP = \frac{(1100)^2 \rho R c_B}{M_{tip}} \int C_D \left[1 - \frac{(m-1)}{m} \frac{M}{M_{tip}} \right] M^3 dM \qquad (8)$$

Substituting in values of C_D and proper limits of integration, one obtains from Equation 8

$$HP = \frac{(1100)^2 \rho Rc_B}{M_{tip}} \int_0^{M_{tip}} \frac{M^2}{10} \left[1 - \frac{(m-1)}{m} \frac{M}{M_{tip}}\right] M^3 dM + \frac{(1100)^2 \rho Rc_B}{M_{tip}} \int_1^{M_{tip}} \frac{1}{10M} \left[1 - \frac{(m-1)}{m} \frac{M}{M_{tip}}\right] M^3 dM \quad (9)$$

$$HP = \frac{(1100)^2 \rho Rc_B}{M_{tip}} \left[\int_0^1 \frac{M^5}{10} dM - \int_0^1 \frac{(m-1)}{mM_{tip}} \frac{M^6}{10} dM + \int_1^{M_{tip}} \frac{M^2}{10} dM - \int_1^{M_{tip}} \frac{(m-1)}{mM_{tip}} \frac{M^3}{10} dM\right] \quad (10)$$

$$HP = \frac{(1100)^2 \rho Rc_B}{10M_{tip}} \left[\frac{1}{6} M^6 \Big|_0^1 - \frac{(m-1)}{7mM_{tip}} M^7 \Big|_0^1 + \frac{1}{3} M^3 \Big|_1^{M_{tip}} - \frac{(m-1)}{4mM_{tip}} M^4 \Big|_1^{M_{tip}}\right] \quad (11)$$

$$HP = \frac{(1100)^2 \rho Rc_B}{10M_{tip}} \left[\frac{1}{6}(1-0) - \frac{(m-1)}{7mM_{tip}}(1-0) + \frac{1}{3}(M_{tip}^3 - 1) - \frac{(m-1)}{4mM_{tip}}(M_{tip}^4 - 1)\right] \quad (12)$$

$$HP = \frac{(1100)^2 \rho Rc_B}{10M_{tip}} \left[\frac{1}{6} - \frac{(m-1)}{7mM_{tip}} + \frac{1}{3} M_{tip}^3 - \frac{1}{3} - \frac{(m-1)}{4m} M_{tip}^3 + \frac{(m-1)}{4mM_{tip}}\right] \quad (13)$$

$$HP = \frac{(1100)^2 \rho R c_B}{10 M_{tip}} \left[M^3_{tip} \left(\frac{1}{3} - \frac{(m-1)}{4m} \right) + \frac{(m-1)}{m M_{tip}} \left(\frac{3}{28} \right) - \frac{1}{6} \right] \qquad (14)$$

where $\rho = 2.377 \times 10^{-3} \quad \frac{\text{slugs}}{\text{ft}^3}$

$R = 1.250$ ft

$c_B = .404$ ft

$m = 4.600$

$M_{tip} = 1.455$

For a single arm blade 59 horsepower is required.

For a double arm blade 118 horsepower is required.

APPENDIX II

MINIMUM SPECIMEN STRENGTH TO DENSITY RATIOS

The following minimum strength-to-density ratios must be met by the test specimen material to insure safe pin attachment to the rotating arm.

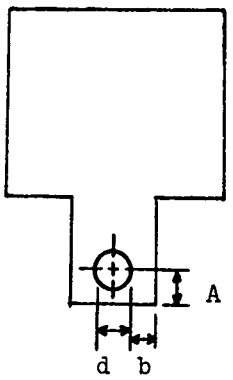

V = Specimen Volume (cu in)
R = Radius of Specimen Arc (in)
W = Angular Velocity of Specimen (rad /sec)
T = Specimen Thickness (in)
F = Stress Concentration Factor
ρ = Specimen Density (lbm /cu in)
S_T = Tensile Strength (lbf /sq in)
S_C = Compression Strength (lbf /sq in)
S_S = Shear Strength (lbf /sq in)

$$\frac{S_T}{\rho} = F\,\frac{VW^2R}{2bT} = \frac{(2)(.11)\left[(2)(3.14)\left(\frac{11640}{60}\right)\right]^2\frac{15.375}{(12)(32.2)}}{(2)(7/32)(0.09)}$$

$$= 330{,}306\ \frac{\text{lbf /sq in}}{\text{lbm /cu in}}$$

$$\frac{S_C}{\rho} = \frac{VW^2R}{Td} = \frac{(2)(.11)\left[(2)(3.14)(11640/60)\right]^2\left(\frac{15.375}{(12)(32.2)}\right)}{(5/16)(0.09)}$$

$$= 231{,}214\ \frac{\text{lbf /sq in}}{\text{lbm /cu in}}$$

$$\frac{S_S}{\rho} = F\,\frac{VW^2R}{2AT} = \frac{(2)(.11)\left[(2)(3.14)(11640/60)\right]^2\left(\frac{15.375}{(12)(32.2)}\right)}{(2)(.276)(0.09)}$$

$$= 261{,}792\ \frac{\text{lbf /sq in}}{\text{lbm /cu in}}$$

REFERENCES

1. Military Specification MIL-E-5007C, Engines, Aircraft, Turbojet and Turbofan, General Specifications For, 30 December 1965.

2. Military Specification MIL-E-5009D, Engines, Aircraft, Turbojet and Turbofan, Tests For, 13 November 1967.

3. Military Handbook 5, 8 February 1966.

4. Design of a High Speed Rain Erosion Tester, PC-1049-M-1, Cornell Aeronautical Laboratory, Inc., 1956.

BIBLIOGRAPHY

Compton, W., McElmury, S., Gulden, M., Smeltzer, C., Mechanisms of Sand and Dust Erosion in Gas Turbine Engines, USAA LABS TR 70-36, August 1970.

Design of a High Speed Rain Erosion Tester, PC-1049-M-1, Cornell Aeronautical Laboratory, Inc., 1956.

Hurley, C., Schmitt, G., Development and Calibration of a Mach 1.2 Rain Erosion Test Apparatus, AFML-TR-70-240, October 1970.

Military Handbook 5, 8 February 1966.

Military Specification MIL-E-5007C, Engines, Aircraft, Turbojet and Turbofan, General Specification For, 30 December 1965

Military Specification MIL-E-5009D, Engines, Aircraft, Turbojet and Turbofan, Tests For, 13 November 1967.

Morris, J., Wahl, N., Supersonic Rain and Sand Erosion Research: Erosion Characteristics of Aerospace Materials, Bell Aerospace Company, AFML-TR-70-265, November 1970.

Supersonic Rain and Sand Erosion Research Progress, Report No. 2, Bell Aerospace Company, May 1970.